Filter-aided extracellular vesicle enrichment (FAEVEr) for proteomics

Jarne Pauwels[1,2], Tessa Van de Steene[1,2], Jana Van de Velde[1,2,3], Freya De Muyer[1,2], Danaë De Pauw[1,2], Femke Baeke [4,5], Sven Eyckerman[1,2] & Kris Gevaert[1,2,$]

[1]VIB-UGent Center for Medical Biotechnology, VIB, 9052 Ghent, Belgium

[2]Department of Biomolecular Medicine, Ghent University, 9052 Ghent, Belgium

[3]Current address: Eurofins Scientific, 9052 Gent, Belgium

[4]Ghent University Expertise Center for Transmission Electron Microscopy and VIB BioImaging Core, 9000 Ghent, Belgium.

[5]Department of Biomedical Molecular Biology, Ghent University, VIB Center for Inflammation Research, 9052 Ghent, Belgium.

[$]Corresponding author: Prof. Dr. Kris Gevaert, VIB-UGent Center for Medical Biotechnology and Department of Biomolecular Medicine, Ghent University, Technologiepark-Zwijnaarde 75, 9052 Ghent, Belgium; e-mail: kris.gevaert@vib-ugent.be

ORCID ID JP: 0000-0002-8525-7109

ORCID ID TVDS: 0000-0001-7915-2055

ORCID ID FDM: 0009-0008-2311-1965

ORCID ID DDP: 0009-0001-4093-6802

ORCID ID FB: 0000-0002-0761-9338

ORCID ID SE: 0000-0001-7525-0096

20 ORCID ID KG: 0000-0002-4237-0283

21

22 # A. Abstract

23 Extracellular vesicles (EVs), membrane-delimited nanovesicles that are secreted by cells into
24 the extracellular environment, are gaining substantial interest due to their involvement in
25 cellular homeostasis and their contribution to disease pathology. The latter in particular has led
26 to an exponential increase in interest in EVs as they are considered to be circulating packages
27 containing potential biomarkers and are also a possible biological means to deliver drugs in a
28 cell-specific manner. However, several challenges hamper straightforward proteome analysis
29 of EVs as they are generally low abundant and reside in complex biological matrices. These
30 matrices typically contain abundant protein concentrations that vastly exceed those of the EV
31 proteome. Therefore, extensive EV isolation and purification protocols are imperative and many
32 have been developed, including (density) ultracentrifugation, size-exclusion and precipitation
33 methods. Here, we describe filter-aided extracellular vesicle enrichment (FAEVEr) as an
34 approach based on 300 kDa MWCO filtration that allows the processing of multiple samples in
35 parallel within a reasonable timeframe and at moderate cost. We demonstrate that FAEVEr is
36 capable of quantitatively retaining EV particles on filters, whilst allowing extensive washing with
37 the mild detergent TWEEN-20 to remove interfering non-EV proteins. The retained particles are
38 directly lysed on the filter for a complete recovery of the EV protein cargo towards proteome
39 analysis. Here, we validate and optimize FAEVEr on recombinant EV material and apply it on
40 conditioned medium as well as on complex serum. Our results indicate that EVs isolated from
41 MCF7 cells cultured with or without serum have a drastic different proteome because of nutrient
42 deprivation.

B. Keywords

Extracellular vesicles, 300 kDa MWCO ultrafiltration, conditioned medium, starvation, EV-depleted serum, TWEEN-20, LC-MS/MS, proteomics

C. Background

Extracellular vesicles (EVs) make up a heterogeneous population of membrane-enclosed particles that are released by virtually all cells into their extracellular (EC) environment and in bodily fluids, such as plasma, urine and cerebrospinal fluid. In general, EVs are subdivided in three main categories according to their biogenesis and size (1). The smallest (30 – 150 nm), termed exosomes, are generated by invaginations at the endosomal membrane, in a transport (ESCRT) dependent (2,3) or independent manner (4). During this process, early endosomes mature into a multivesicular body (MVB) that holds multiple membrane delineated vesicles termed intraluminal vesicles (ILVs). Once the MVB fuses with the plasma membrane (PM), these ILVs are released into the EC environment as exosomes. Microvesicles (100 – 500 nm) are formed by an immediate outward budding of the PM, orchestrated by the ESCRT machinery (5). These protrusions are ultimately pinched off and released from the cell. Finally, apoptotic bodies (50 – 5,000 nm) are formed during apoptotic cell disassembly with large extrusions at the PM, fragmenting dying cells in large blobs that may even contain organelles (6). Ultimately, in the body, different EV categories are released from millions of individual cells, forming an immensely heterogeneous EV pool. This also results in the loss of information on their biogenesis and therefore, in practice, EVs are distinguished from one another by their size; small (sEV, < 200 nm) or large (lEV, > 200 nm), as described in the MISEV2018 guidelines (7). Note that since there is a certain level of size overlap between the different subtypes, none of these subpopulations is exclusive for either the small or the large EV group (8).

66 Due to their biogenesis, EVs have some important biophysical properties. First, EVs are
67 delineated by a phospholipid bilayer, effectively shielding their cargo (consisting of proteins,
68 oligonucleotides (RNA & DNA), lipids and metabolites) from the hostile extracellular
69 environment, thereby, maintaining the functionality and stability of biomolecules (9). Therefore,
70 the cargo can be considered to represent the molecular state of the parental cell at the moment
71 of EV formation. In addition, (trans)membrane proteins are incorporated into the lipid bilayer,
72 which, in turn, allows targeted signal transduction with distant EV receiving cells and/or allows
73 the selective delivery of their cargo in such cells (10,11). In physiological conditions, this cargo
74 takes part in cellular communication and homeostasis (12,13). In disease, however, the EV cargo
75 can contribute to the pathology, for example by initiating a pre-metastatic niche at a distant
76 location during cancer progression (14,15).

77 Both of these EV characteristics are appealing for clinical implementations, offering great
78 potential for both therapeutic applications (i.e. targeted drug delivery) as well as for biomarker
79 discovery (e.g. disease diagnosis, prognosis and therapy guidance) (16–18). Although the
80 therapeutic applications remain rather hypothetical or, at best, experimental to date (19,20), the
81 biomarker potential of circulating EVs has known a substantial increase in the past decade.
82 Indeed, EVs are present in different biofluids, such as plasma and urine, which can be isolated
83 in a low to non-invasive way at multiple time points.

84 In general, considering the biophysical properties of EVs, the identification and characterization
85 of protein biomarkers within or on circulating EVs from liquid biopsies might lead to (early)
86 disease diagnosis, monitoring of disease progression and therapeutic response, all critical
87 aspects towards the establishment of precision treatment (21). In this respect, EVs have shown
88 clinical potential as a source of circulating biomarkers for different cancers (e.g. breast (18),

89 urinary tract (22) and bone cancer (23)) and other diseases such as Alzheimer's disease (24,25),
90 chronic liver disease (26) and multiple sclerosis (27).

91 Unfortunately, multiple challenges complicate EV protein research, especially with regard to
92 proteome analysis by bottom-up mass spectrometry (MS), which is the method-of-choice for
93 unbiased protein biomarker discovery (28). Indeed, once EVs are released by the cell they form
94 a heterogeneous pool that resides in biological complex matrices that contain proteins at levels
95 that exceed those of the low abundant EV proteins by several orders of magnitude (29), such as
96 albumin in plasma and uromodulin in urine. In addition, they co-exist with non-EV particles that
97 overlap in size and density such as apolipoprotein particles. As a result, an adequate EV
98 enrichment and purification strategy remains essential for in-depth EV-associated biomarker
99 discovery (30). Of note, in MS-based proteomics, the recent advent of data-independent
100 acquisition (DIA) MS due to computational (31,32) and instrumental (33) improvements has
101 proven to cope more successfully with the above-mentioned challenges compared to traditional
102 data-dependent acquisition (DDA), as it is less biased to relative high protein levels.

103 Over the years, different EV enrichment strategies have been developed to enrich, purify and
104 concentrate EVs for in-depth proteome analysis and quantitative profiling, with the most
105 prominent strategies being based on size (ultracentrifugation and size-exclusion
106 chromatography) (34,35), density (density gradient ultracentrifugation) (36), precipitation (37,38)
107 or capture of molecular markers present on the EV surface (immuno-capture) (39). To further
108 enhance the purity of EV preparations, different orthogonal approaches can be combined (40,41).
109 However, a golden standard is yet to be determined, as the different strategies not only differ in
110 the consumption of resources and time, but also in terms of effectiveness and reproducibility.
111 Indeed, the different EV isolation techniques introduce variation between experiments in terms
112 of EV count and heterogeneity of molecular (protein) cargo. This has been emphasized in

113 different studies in which EV enrichment strategies were compared (42–46). Along this line,
114 initiatives such as MISEV and EV-TRACK were established within the EV research community to
115 encourage transparency on experimental procedures used to enrich EVs and on acquired
116 results, thereby enhancing inter-lab reproducibility (7,47). Importantly, purified, recombinant
117 EVs are now used as biological reference material to monitor technique development and
118 reproducibility, and improve data normalization (48,49). However, all enrichment strategies have
119 one major bottleneck in common; they lack the possibility for parallelization and high-
120 throughput set-ups. Indeed, enrichment strategies such as (density gradient) ultracentrifugation
121 require (multiple) lengthy centrifugation steps, are generally limited to six or eight samples and
122 require expensive instrumentation. Size-exclusion chromatography (SEC) often requires a
123 concentration step both prior and after EV enrichment and, in addition, also validation (often by
124 Western blotting) to identify those fractions containing EV material (50). Commercial EV
125 enrichment kits are again expensive and, more importantly, show high variability between
126 suppliers (51,52).

127 Ultrafiltration (UF) has thus far been mainly used as an intermediate step in EV enrichment
128 strategies to reduce the volume of conditioned medium or liquid biopsy either prior (e.g. density
129 gradient ultracentrifugation) or after EV enrichment (e.g. SEC) (53–55). The main challenges
130 associated with ultrafiltration for EV proteome analysis are the inefficient removal of non-EV
131 proteins, irreversible blocking of the filter membrane and low recovery of the retained particles
132 (56,57). However, it also offers inherent advantages, such as the limited cost, reduced sample
133 preparation time and the potential of analyzing multiple samples simultaneously using standard
134 lab equipment. In addition, UF has little bias towards EV subpopulations (58), in contrast to (for
135 instance) immuno-capture.

136 Here, we propose an ultrafiltration strategy for the isolation and purification of EVs from
137 conditioned medium and bovine serum, which we termed filter-aided extracellular vesicle
138 enrichment or FAEVEr. In short, pre-cleared conditioned medium or serum is loaded on 300 kDa
139 MWCO filters and centrifuged briefly at a moderate speed during which EVs are retained on the
140 filter, whereas the bulk of globular (non-EV) proteins do not. Remaining filter-retained non-EV
141 proteins are removed through subsequent purification steps that include TWEEN-20-containing
142 wash buffers. The retained (purified) EVs are then efficiently lysed on the filter in SDS-containing
143 buffer and the EV lysates are conveniently collected by centrifugation and processed for
144 proteomics applications, such as Western blotting and LC-MS/MS analysis. Recombinant EV
145 (rEV) material isolated from HEK293T conditioned medium was used for testing and optimizing
146 our strategy for comparison to ultracentrifugation, the most widely implemented EV enrichment
147 strategy. We demonstrate that the EV purity is considerably improved when including TWEEN-
148 20 in the wash steps without jeopardizing EV integrity, even at high concentrations of the
149 detergent. We then successfully applied FAEVEr to complex biofluids (bovine serum) and
150 investigated the effect on the EV protein cargo when using serum-depleted medium on MCF7
151 cell cultures.

152

153 # D. Material and methods

154 ## 1. Cell culture

155 All cell culture experiments were performed using standard protocol and lab equipment.

156 ### a. rEV production

157 A complete protocol for the transformation and production of recombinant extracellular vesicles
158 (rEV) material is described in (49,59). In short, approximately 4 million HEK293T cells of low
159 passage number (< 10) were seeded in a T75 falcon with Dulbecco's Modified Eagle Medium
160 (DMEM, Gibco) containing 10% standard FBS and incubated for 48 h at 37 °C in 5% CO_2. The
161 HEK293T cells were transfected by adding a mixture of polyethyleneimine (PEI) and the DNA bait
162 construct (12x, pMET7- GAG-eGFP) in DMEM + 2% FBS for 6 h at 37 °C in 5% CO_2. The medium
163 was then discarded and replaced with 8 mL fresh DMEM supplemented with 10% EV-depleted
164 FBS (EDS, Thermo A2720801). After 48 h incubation at 37 °C in 5% CO_2, cell transfection was
165 evaluated under UV light (excitation at 488 nm and emission at 507 nm) before the conditioned
166 medium (CM) was isolated. The CM was immediately pre-cleared by centrifugation at 1,000 x g
167 for 10 min and filtration of the supernatant using 0.22 µm filters (Millex). The pre-cleared CM
168 was divided over different aliquots and frozen in -80°C until further use. Note that pure rEV
169 extracts are commercially available (SAE0193, Sigma-Aldrich).

170 ### b. MCF7 cells

171 MCF7 cells of low passage number (< 10) were cultured using a standard protocol and equipment.
172 The cells were seeded in T75 flasks with DMEM containing 10% standard FBS and incubated at
173 37 °C in 5% CO_2. When the cells reached 70-80% confluence, the medium was discarded and the

174 cells were washed three times with PBS. Experiments were performed in duplicate, adding 8
175 mL of DMEM supplemented with either 0%, 2%, 5% or 10% EDS (Thermo, A2720801) or OptiMEM
176 supplemented with 0% EDS. After 24 h, the CM containing 0% EDS were isolated, whereas the
177 2%, 5% and 10% EDS containing CM were isolated after 48 h. The CM was immediately pre-cleared
178 by two centrifugation rounds (500 x g for 5 min, and 10,000 x g for 10 min, room temperature)
179 and filtration using 0.22 µm filters (Millex).

180 2. EV enrichment

181 a. Ultrafiltration using 300 kDa MWCO filters

182 Pre-cleared CM was diluted 1:1 with PBS with or without supplemented TWEEN-20 and vortexed
183 for 5 – 10 s. The final volume was then transferred to 300 kDa MWCO polyethylene sulfone (PES)
184 filters (Vivaspin®6, Sartorius VS0652) and centrifuged. Centrifugation was done for 10 – 15 min
185 at room temperature either at 6,000 x g for fixed angle rotors (F14x50cy, Sorvall Lynx 4,000,
186 Thermo) or at 4,000 x g for swing-out rotors (e.g. A-4-44, 5804R, Eppendorf). The filter retentate
187 was washed several times with wash buffer (PBS with or without supplemented TWEEN-20) and
188 centrifuged for 5 – 7 min per wash step. After three rounds of washing, the retained particles
189 were either solubilized from the filter for nanoparticle tracking analysis or electron microscopy,
190 or immediately lysed on the filter for maximal recovery of the proteome. For recovery, 500 µL
191 50 mM HEPES was added on the filter and vortexed for 10 – 15 sec after which the solution was
192 transferred to a fresh tube and vacuum-concentrated (SpeedVac). To immediately collect the EV
193 lysate, 5% SDS in 50 mM TEAB is added and collected after 15 min incubation (37°C, 500 rpm) by
194 centrifugation (5 min at room temperature).

195 b. Ultracentrifugation

196 Pre-cleared conditioned medium was transferred to polycarbonate thick-wall tubes (Beckman,
197 343778) and centrifuged for 90 min at 100,000 x g (4°C) using a Optima TLX ultracentrifuge
198 equipped with a TLA-120.2 rotor (Beckman). The supernatant was carefully removed and the
199 pellet washed with PBS with or without TWEEN-20 before a second round of ultracentrifugation
200 for 90 min at 100,000 x g (4°C). Again, the supernatant was carefully removed and the pellets
201 were either solubilized for NTA or EM, or immediately lysed for maximal recovery of the
202 proteome. The EVs were lysed by adding 5% SDS in 50 mM TEAB and the lysate collected after
203 15 min incubation (37 °C, 500 rpm).

204 3. Proteomics

205 a. Western blot

206 Samples for Western blot analysis were incubated for 5 min at 95 °C with XT sample buffer (4x)
207 and XT reducing agent (20x) (BioRad). The protein material was separated by SDS-PAGE (4%-
208 12%) for 80 min at 120 V prior to transfer onto a PVDF membrane (100 V, 30 min). The membrane
209 was incubated overnight at 4 °C with primary antibodies (rabbit monoclonal anti-Calnexin
210 (ab133615) and mouse monoclonal anti-HIV p24 39/5 4A (ab9071); 1:1,000). The next day, the
211 membrane was washed several times before incubation for 1 h at room temperature with
212 secondary antibodies (goat anti-rabbit IRDye 680 CW and goat anti-mouse IRDye 800 CW;
213 1:10,000). Visualization was done on an Odyssey infrared imager (v3.0.16, LI-COR Biosciences).

214 b. LC-MS/MS sample preparation

215 The proteome was prepared for LC-MS/MS analysis using S-Trap™ mini columns (ProtiFi, C02-
216 mini-80) using the manufacturer's protocol. In brief, proteins in lysis buffer (5% SDS 50 mM
217 TEAB, pH 7.4) were reduced and alkylated using 5 mM TCEP (10 min at 55 °C) and 20 mM
218 iodoacetamide (IAA, 10 min at room temperature in the dark), respectively. The sample was
219 acidified to 1.2% phosphoric acid and diluted seven-fold with binding/wash buffer (90% methanol
220 in 100 mM TEAB, pH 7.4). The samples were transferred to the corresponding S-Trap™ columns
221 and each time centrifuged at 4,000 x g for 30 s during sample loading and washing. For protein
222 digestion, 0.5 µg of trypsin (Promega, V5111) was added to 125 µL 50 mM TEAB (pH 7.4) and
223 samples were incubated overnight at 37 °C. The next day, the peptides were recovered by
224 sequential elution by centrifugation (4,000 x g for 30 s at room temperature) using 80 µL 50 mM
225 TEAB (pH 7.4), 80 µL 0.2% formic acid and 80 µL of 50% acetonitrile (ACN), 0.2% formic acid in
226 dH_2O. The eluates (app. 365 µL) were transferred to MS vials, vacuum-dried in a SpeedVac and
227 stored at -20 °C. We have submitted all relevant data of our experiments to the EV-TRACK
228 knowledgebase (EV-TRACK ID: EV240045) [34].

229 c. LC-MS/MS analysis

230 Purified peptides were re-dissolved in loading solvent A (0.1% TFA in water/ACN (98:2, v/v)) and
231 the peptide concentration was determined on a Lunatic instrument (Unchained Lab). For each
232 sample the injection volume was adjusted to inject equal amounts of peptide material (500 ng)
233 for LC-MS/MS analysis on an Ultimate 3000 RSLCnano system in-line connected to a QExactive
234 Exploris (for optimization and validation) or an Orbitrap Fusion Lumos mass spectrometer
235 (Thermo) (MCF7 cells and EVs). QCloud was used to control instrument longitudinal performance
236 during the project [57, 58]. The mass spectrometry proteomics data have been deposited to the

237 ProteomeXchange Consortium via the PRIDE [59] partner repository with the dataset identifiers
238 PXD051938 (comparison FAEVEr with UC), PXD051955 (comparison MCF7 proteome of EVs and
239 cells under starving conditions) and PXD051956 (comparison FBS with EDS).

240 LC-MS/MS analysis using the Fusion Lumos instrument

241 LC-MS/MS data-independent (DIA) acquisition on the Fusion Lumos was initiated by trapping
242 the peptide material at 20 µl/min for 2 min in loading solvent A on a Pepmap column (300 µm
243 internal diameter (I.D.), 5 µm beads, C18, Thermo). The peptides were separated on a 110 cm µPAC
244 prototype column (Thermo), kept at a constant temperature of 50 °C. Peptides were eluted by a
245 non-linear gradient starting from 2% MS solvent B (0.1% formic acid (FA) in acetonitrile), reaching
246 26.4% MS solvent B in 82 min and 44% MS solvent B in 90 min and 56% MS solvent B in 100 min
247 starting at a flowrate of 600 nl/min for 5 min, and completing the run at a flow rate of 300 nl/min,
248 followed by a 5-minute wash at 56% MS solvent B and re-equilibration with MS solvent A (0.1%
249 FA in water). The mass spectrometer was operated in data-independent mode. Full-scan MS
250 spectra ranging from 400-900 m/z with a target value of 4E5, a maximum fill time of 50 ms and
251 a resolution of 60,000 were followed by 50 quadrupole isolations with a precursor isolation width
252 of 10 m/z for HCD fragmentation at an NCE of 34% after filling the trap at a target value of 4E5
253 for maximum injection time of 54 ms. MS2 spectra were acquired at a resolution of 30,000 at
254 200 m/z in the Orbitrap analyser without multiplexing. The isolation intervals ranged from 400 –
255 900 m/z, without overlap.

256 LC-MS/MS analysis using the Orbitrap Exploris 240 instrument

257 The peptide material was injected for LC-MS/MS analysis on a Vanquish™ Neo UHPLC System
258 in-line connected to an Orbitrap Exploris 240 mass spectrometer (Thermo). Injection was
259 performed in trap-and-Elute workflow in combined Control mode (maximum flow of 60 µl/min

260 and maximum pressure of 800 bar) in weak wash solvent (WW, 0.1% trifluoroacetic acid in
261 water/acetonitrile (ACN) (99.5:0.5, v/v)) on a 5 mm trapping column (Thermo scientific, 300 µm
262 internal diameter (I.D.), 5 µm beads). The peptides were separated on a 250 mm Aurora Ultimate,
263 1.7µm C18, 75 µm inner diameter (Ionopticks) kept at a constant temperature of 45 °C. Peptides
264 were eluted by a gradient starting at 0.5% MS strong wash solvent (SW) (0.1% FA in acetonitrile)
265 reaching 26% MS SW in 30 min, 44% MS SW in 38 min, 56% MS SW in 40 min followed by 5-minute
266 wash at 56% MS SW and column equilibration in Pressure Control mode (separation column:
267 fast equilibration, maximum pressure of 1500 bar, equilibration factor=2; Trap column: fast wash
268 and equilibration, wash factor=100) with MS WW . The flow rate was set to 300 nl/min. The mass
269 spectrometer was operated in data-independent mode, automatically switching between MS and
270 MS/MS acquisition. Full-scan MS spectra ranging from 400-900 m/z with a normalized target
271 value of 300%, a maximum fill time of 25 ms and a resolution at of 60,000 were followed by 30
272 quadrupole isolations with a precursor isolation width of 10 m/z for HCD fragmentation at an
273 NCE of 30% after filling the trap at a normalized target value of 2000% for maximum injection
274 time of 45 ms. MS2 spectra were acquired at a resolution of 15,000 with a scan range of 200-
275 1800 m/z in the Orbitrap analyser without multiplexing. The isolation intervals were set from 400
276 – 900 m/z with a width of 10 m/z using window placement optimization. EASY-IC™ was used in
277 the start of the run as Internal Mass Calibration

278 d. Database searching and data analysis

279 Data-independent acquisition (DIA) spectra were searched with the DIA-NN software (v1.8.2b)
280 [60] in library-free mode against the combination of two protein databases downloaded from
281 Swiss-Prot; the complete human protein sequence database (January 2021, 20,394 sequences)
282 supplemented with bovine serum protein sequences (March 2021, 618 sequences). For searches
283 that included rEV material, we included the Gag-eGFP protein sequence as well. The mass

284 accuracy was set to 10 ppm and 20 ppm for MS1 and MS2, respectively, with a precursor FDR of
285 0.01. Enzyme specificity was set to trypsin/P with a maximum of two missed cleavages. Variable
286 modifications were set to oxidation of methionine residues (to sulfoxides) and acetylation of
287 protein N-termini. Carbamidomethylation of cysteines was set as a fixed modification. The
288 peptide length range was set to 7-30 residues with a precursor charge state between 1 and 4
289 and an m/z range between 400-900 and 200-1,800 for the precursor and fragment ions,
290 respectively. Cross-run normalization was set to RT dependent with the quantification strategy
291 set to high accuracy and the neural network classifier to single-pass mode. The result file was
292 further processed in KNIME (v4.3.3) by removing non-proteotypic peptides and identifications
293 with a protein q-value above 0.01. Peptide quantifications were aggregated to protein group
294 quantifications using the median of the corresponding normalized LFQ values. Further data
295 analysis was performed with Perseus (version 1.6.14.0), GraphPad Prism (v9.4.1) and RStudio
296 (2023.12.1).

297 For the analysis of the EV and cellular proteomes across different experimental conditions,
298 proteins that were significantly differentially abundant were identified by multiple sample testing
299 (ANOVA) and selected for hierarchical clustering (Euclidean distance with averaged linkage)
300 after Z-scoring the individual proteins over the different conditions. Row clusters were defined
301 manually and used for gene ontology (GO) enrichment against the corresponding initial database
302 and included biological process (GOBP), molecular function (GOMF), cellular component (GOCC)
303 annotations and KEGG pathways. GO term enrichment was done using the online WebGestalt
304 tool for Gene ontology enrichment (GOA) (60).

305 ## 4. EV characterization

306 ### a. NTA analysis

307 Recuperated EV particles were diluted to 1 mL using PBS (pH 7), injected in a calibrated Zetaview
308 and analyzed with the corresponding software package (version 8.05.16 SP2). The temperature
309 was maintained at 23°C and the analysis was done at a sensitivity of 70 and a shutter of 100 for
310 3 cycles at 60 fpm. The results were plotted and analyzed in GraphPad Prism (v10.2.2)

311 ### b. Scanning electron microscopy

312 Filters containing EVs were placed in 2 ml Eppendorf tubes and fixed with 4% paraformaldehyde
313 and 2% glutaraldehyde in 0.1 M Sodium cacodylate buffer at room temperature. After one hour,
314 the fixative was replaced and filters were washed 3 times for 5 min with dH_2O. After dehydration
315 in 30%, 50%, 70%, 95% and 2x 100% ethanol for 30 min each, the filters were critical point dried
316 (EM CPD300, Leica) and imaged on a Crossbeam 540 SEM (Zeiss) at 1kV.

317 ### c. Transmission electron microscopy

318 Aliquots (5 µl) of the EV solutions were blotted for 1 min on formvar- and carbon-coated Ni maze
319 grids (EMS), which were glow discharged for 40 sec at 15 mA. The grids were then washed five
320 times in droplets of dH_2O and stained in a droplet of 1/4 Uranyl Acetate Replacement Stain (EMS)/
321 dH_2O for 1 min. Excess stain was removed with filter paper and the grids were air dried for at
322 least four hours before viewing with the TEM. Imaging was done at 80kV on a JEM1400plus
323 (JEOL).
324

325 ## E. Result section

326 ### 1. Use of 300 kDa MWCO filters to enrich EVs

327 Although ultrafiltration is a valid and well-implemented method to concentrate intact EVs, it
328 holds many challenges as a stand-alone EV enrichment strategy. Nevertheless, ultrafiltration
329 also has important advantages such as low cost and fast processing times, and it does not
330 require specific instrumentation compared to, for instance, ultracentrifugation.

331 Here, we introduce Filter-Aided Extracellular Vesicle Enrichment (FAEVEr), a strategy that uses
332 300 kDa MWCO polyether sulfone (PES) filters to purify and concentrate intact EVs (Figure 1). In
333 brief, pre-cleared conditioned media or biofluids are transferred onto the 300 kDa MWCO filter
334 membrane and centrifuged at moderate speed (4,000 – 6,000 x g), retaining the EV particles on
335 the filter (retentate) whereas globular non-EV proteins are removed (filtrate). By including three
336 consecutive wash steps, non-EV proteins are increasingly removed, by which the EV retentate
337 is further purified. Eventually, by using a lysis buffer with high percentages (5%) of SDS, EVs
338 undergo efficient lysis and their cargo is conveniently recovered by centrifugation. The EV
339 sample is then further processed for proteomics using S-Trap columns (61). Here, we opted for
340 PES membranes, as filters based on such membranes are hydrophilic with low protein
341 adsorption characteristics. In addition, PES material is resistant against high pH ranges and
342 temperatures and can withstand a wide variety of solvents, buffers and detergents.

343 Recombinant EV (rEV) material was used for the initial optimization of the 300 kDa MWCO
344 ultrafiltration strategy as it has similar biochemical and biophysical characteristics as sample
345 EVs (48). The rEV material is derived from the conditioned medium of HEK293T cells, cultured in
346 10% EV-depleted serum, that overexpress the Gag-eGFP fusion protein (49). The Gag subunit

347 multimerizes at the plasma or endosomal membrane and initiates membrane curving, resulting
348 in the formation of microvesicles and intraluminal vesicles, respectively, commonly referred to
349 as virus-like particles (59,62) (**Error! Reference source not found.**). As a result, secreted rEV
350 material is overrepresented in the conditioned medium and contains high levels of luminal Gag-
351 eGFP, enabling the evaluation of EV integrity during the consecutive FAEVEr steps.

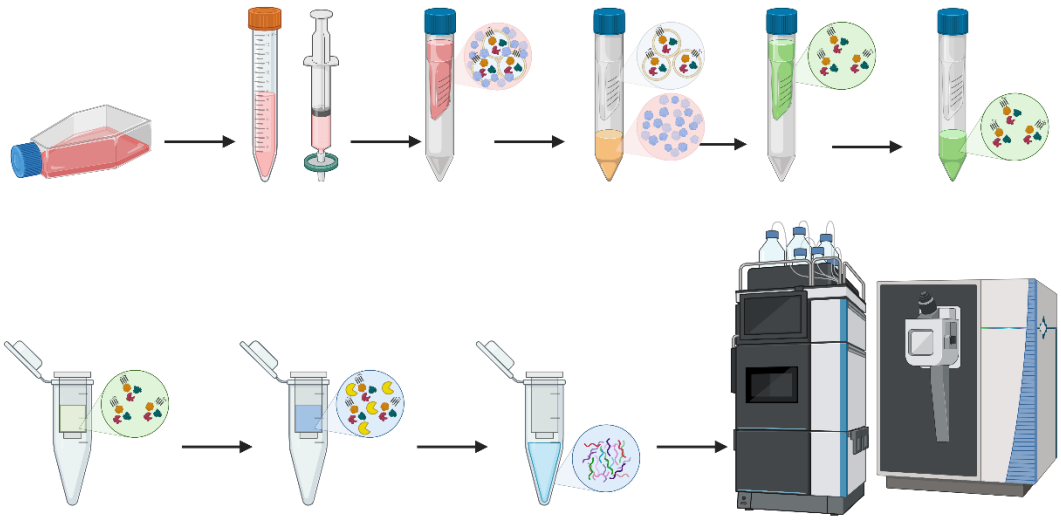

352

353 **Figure 1: Schematic overview of the FAEVEr workflow.** Conditioned media or biofluids are
354 precleared and transferred onto the 300 kDa MWCO PES filter (red). Driven by centrifugation,
355 the globular proteins pass through the filter (orange), whereas the EV particles are
356 quantitatively retained (grey). The retentate is subsequently washed three times using PBS
357 supplemented with TWEEN-20 to further increase the EV purity. Ultimately, intact particles are
358 recovered for qualitative analysis, or lysed (green) immediately on the filter. The lysate is
359 recovered by centrifugation and prepared for proteomic applications (e.g. LC-MS/MS analysis
360 or Western blotting). Figure created in Biorender.

361 We confirmed that rEV particles are retained on the 300 kDa MWCO mesh using scanning
362 electron microscopy (SEM) (Figure 2A and **Error! Reference source not found.**), indicating that
363 ultrafiltration is an efficient EV enrichment strategy. Indeed, after completing the FAEVEr
364 protocol, rEV particles were recovered from the filter for nanoparticle tracking analysis (NTA)
365 (Figure 2B) and transmission electron microscopy (TEM) characterization (Figure 2C). However,
366 in line with Vergauwen *et al.* (56), we noticed that the quantitative recuperation of particles from
367 the filter PES membrane is variable and that not all particles are recovered. When the remaining
368 rEV fraction on the filter was lysed and analyzed on Western blot, we observed that a substantial
369 share of the rEV material fails to be solubilized and remains on the filter (Figure 2D).

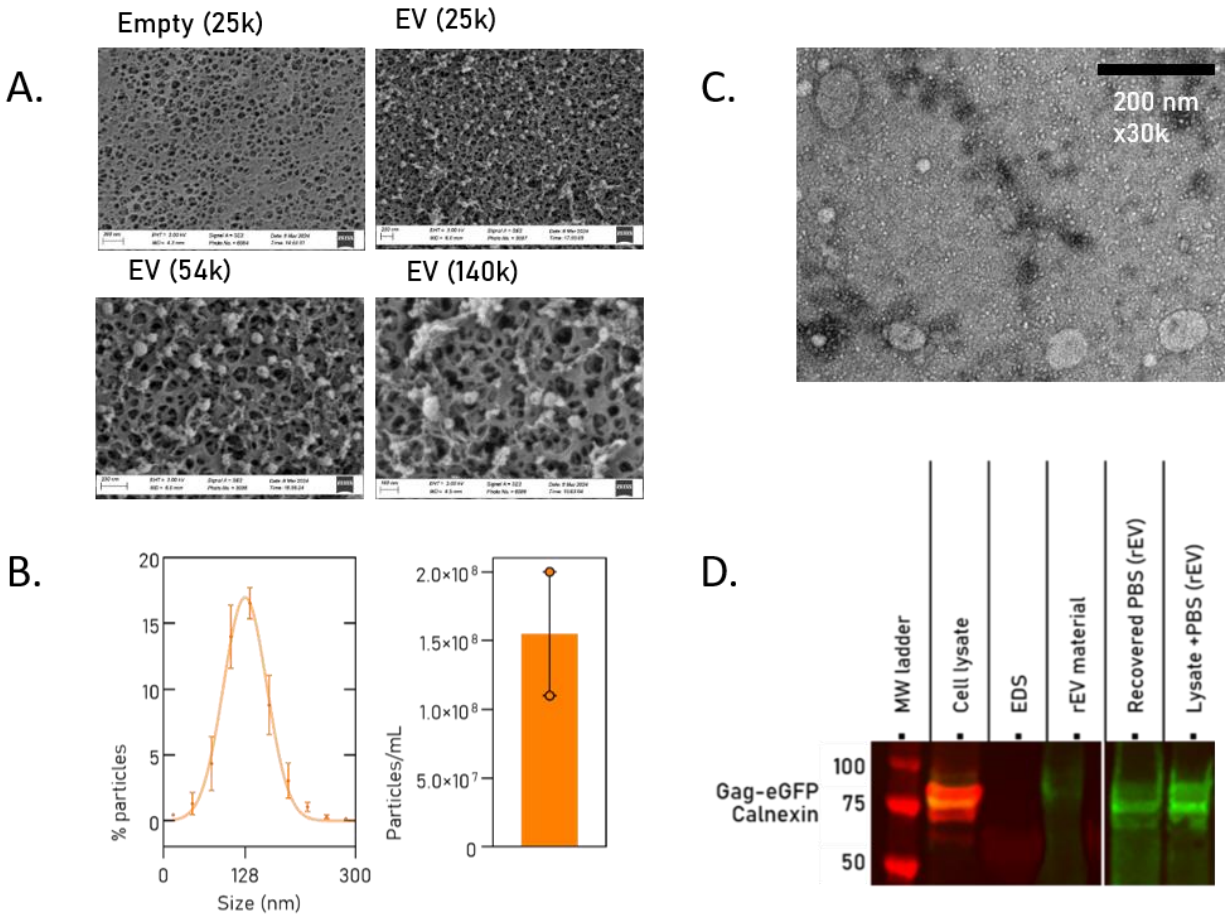

370

371 **Figure 2: Qualitative analysis of FAEVEr retained particles.** A) Scanning electron microscope of
372 an empty filter and after rEV enrichment. B) EV size distribution and count, and transmission
373 electron microscopy (C) of recovered rEV particles from the filter. D) Western blot reveals
374 incomplete recuperation of rEV particles from the filter. EDS: EV-depleted serum (negative
375 control), rEV material: commercial rEV particles (positive control), PBS: phosphate-buffered
376 saline washed rEV particles.

377 Concluding this part, we found that FAEVEr is an efficient approach for isolating EV particles
378 from conditioned medium for downstream proteome analysis and that we can successfully
379 recuperate intact particles from the filter (56). By immediately lysing the filter-retained EV
380 material using high percentages of SDS for proteomic applications, we ensure EV lysis,
381 comprehensive solubilization of (membrane) proteins (63) and maximal protein recovery. Note
382 that SDS is irreconcilable with LC-MS/MS analysis and we therefore introduced S-Trap columns
383 in our workflow (61,64). The S-Trap protocol is easy, fast and reproducible and has been
384 extensively compared to other methods in different studies (65,66).

385 ## 2. Comparison of FAEVEr to ultracentrifugation

386 Using EV proteome analysis, we set out to compare our FAEVEr approach with
387 ultracentrifugation (UC), the most used strategy for EV enrichment. rEV material was isolated,
388 pre-cleared and divided over different aliquots before subjecting it to the corresponding EV
389 enrichment strategy in triplicate. In terms of sample preparation, the overall sample preparation
390 time differs noticeably. Ultracentrifugation required at least two rounds of centrifugation,
391 totaling to 3 h of centrifugation time, whereas FAEVEr was finished within the hour, including
392 centrifugation steps and hands-on time.

393 For an in-depth analysis of the proteome results, we examined the occupancy of the LC-MS/MS
394 spectral space, which is a measure of the recorded spectra and allows us to differentiate
395 between recorded spectra of bovine and human origin. Our results indicate that the relative
396 spectral space occupancy by bovine precursors was slightly reduced (from 35% to 30%) using
397 FAEVEr compared to UC (Figure 3A). In addition, approximately 15% more proteins were
398 identified proportionally distributed over the different cellular locations (Figure 3B). The six
399 commonly used EV markers are well represented and identified with similar relative intensities
400 between strategies (Figure 3C) and 85% of the identified proteins by the UC were found by
401 FAEVEr (Figure 3D). In addition, the same trend was observed for the number of unique peptides
402 (13%) and the number of the associated peptide-spectral matches (PSMs), the number of
403 recorded spectra that were translated in a confident peptide identification (14%) (Figure 3E).
404 Importantly, we observed a large decrease in the accompanying coefficient of variance (%CV)
405 for FAEVEr between the replicates as well as fewer missing values, which results in an
406 increased data completeness and therefore higher reproducibility with more accurate protein
407 quantifications (Figure 3F). From this experiment, we can thus conclude that ultrafiltration using
408 300 kDa MWCO filters allows for EV enrichment and is comparable to UC in terms of EV proteome
409 depth.

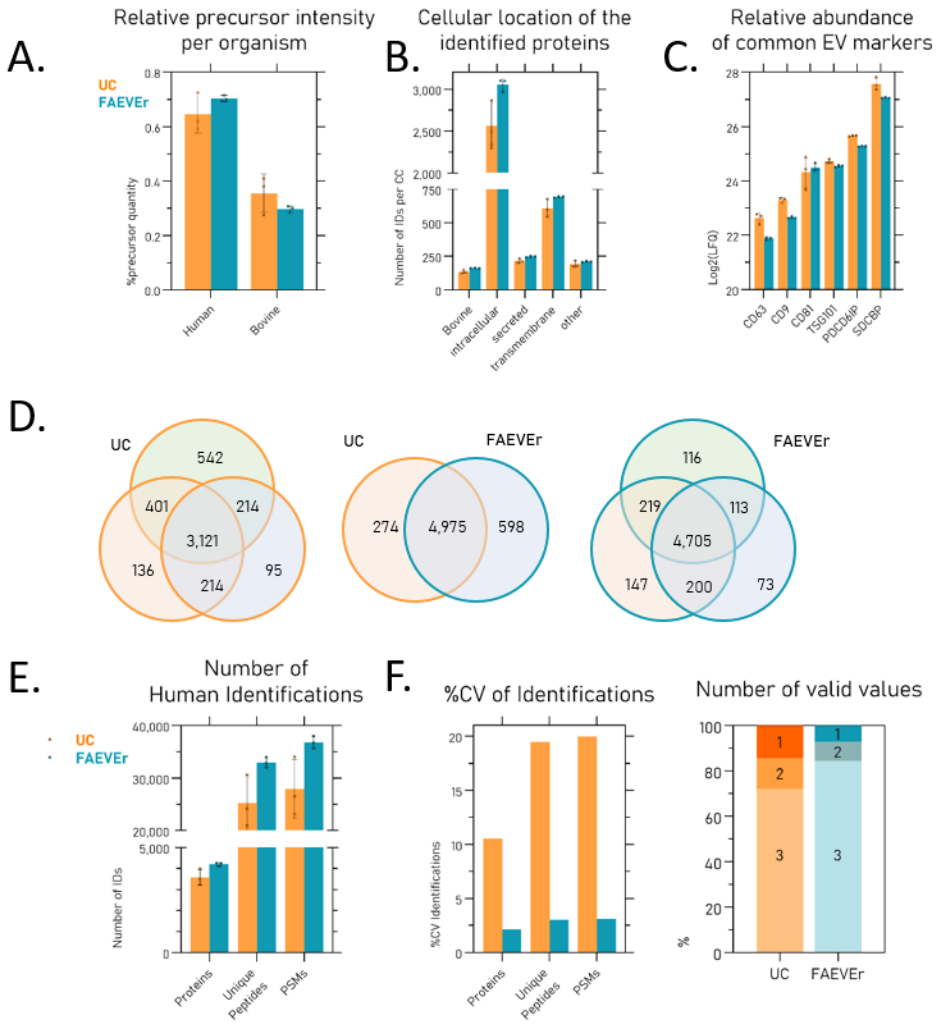

Figure 3: Overview of the comparison between FAEVEr and ultracentrifugation. A) Comparison of the relative abundance of precursor material from bovine or human origin. B) Distribution of the protein identifications across the cellular localizations of the parental cell. C) High relative abundance of six molecular EV markers. D) Overlap of protein identifications between UC and FAEVEr. E) Total number of identified human proteins, identified unique peptides and peptide-spectral matches from these proteins between UC and FAEVEr. F) Decreased relative variance (%CV) and fewer missing values are observed with FAEVEr compared to UC. UC: ultracentrifugation (orange), FAEVEr: Filter-aided EV enrichment (teal), CC: cellular

419 compartment, LFQ: label-free quantification intensity, PSM: peptide-spectral match, %CV:
420 coefficient of variance.

421 3. TWEEN-20 improves the removal of non-EV proteins

422 One major pitfall of ultrafiltration is the inefficient removal of non-EV proteins, which has a
423 detrimental effect on the numbers of identified and quantified EV proteins following LC-MS/MS
424 analysis. Therefore, we explored the use of mild detergents to minimize the interaction between
425 proteins and the filter membrane. However, as EVs are delineated with a lipid bilayer and
426 therefore susceptible to detergent-mediated lysis, caution should be taken with the choice and
427 concentration of the detergent. A study by Osteikoetxea *et al.* explored the minimal concentration
428 of different detergents required for efficient lysis of EV particles in solution (67) and found that
429 this concentration greatly depends not only on the detergent used, but also on the EV
430 subpopulation (exosomes, microvesicles and apoptotic bodies). In particular, the smallest
431 population (exosomes) demonstrated increased resilience against detergents compared to
432 larger vesicles (microvesicles and apoptotic bodies) due to an increase in liquid order because
433 of an accumulation of cholesterol and sphingolipids during their formation (68–70). In their work,
434 Osteikoetxa *et al.* demonstrate that EVs are generally efficiently lysed even at low percentages
435 of SDS, Triton X-100 or sodium deoxycholate. On the contrary, an exceptional high tolerance is
436 observed towards TWEEN-20, a rather mild detergent that is commonly used in other
437 biochemical assays such as Western blotting to reduce unwanted adsorption of protein material
438 to membranes (71) and thereby decreases irreversible or total membrane fouling (72,73).
439 TWEEN-20 was explored here as an additive to improve the efficiency of the washing steps and
440 thus removal of non-EV proteins during the enrichment of EVs whilst keeping EVs intact. The
441 efficiency of washes with TWEEN-20-containing buffers was tested by Coomassie staining of the

442 different filtrate fractions of conditioned medium after completing the FAEVEr protocol using 0%,
443 0.1%, 0.5%, 1%, 2% and 5% TWEEN-20 in the wash buffer. We observed that PBS-only (the 0%
444 TWEEN-20) condition is not capable of removing the bulk of bovine serum albumin (BSA; 65 kDa),
445 whereas BSA-bands are more intense in the TWEEN-20 supplemented wash fractions. In
446 addition, upon recovery of the retained material by lysis in 5% SDS, we observed an intense band
447 for the PSB-only condition, which was absent in the TWEEN-20 supplemented ones (**Error!**
448 **Reference source not found.**). This suggested that TWEEN-20 is indeed capable of removing the
449 bulk of (contaminating) bovine serum material from the filter membrane and therefore should
450 result in an EV proteome fraction that is more pure.

451 Next, we validated this beneficial effect of TWEEN-20 in wash buffers using rEV material, which
452 also allows us to validate the integrity of the particles as they contain the Gag-eGFP protein on
453 the luminal side. We thus argued that, when the rEV particles remain intact, no luminal Gag-
454 eGFP should be present in the filtrates. In short, pre-cleared conditioned medium containing rEV
455 material was filtered (300 kDa MWCO) and washed several times with up to 5% TWEEN-20 in
456 PBS. After each centrifugation step, the filtrate was collected and the presence of luminal Gag-
457 eGFP validated on Western blot, shown in Figure 4A. The almost complete absence of luminal
458 Gag-eGFP in the flow-through and washes (1-3) does not only indicate that intact rEV particles
459 are retained on the filter, but also that they maintain their integrity in concentrations up to 5%
460 TWEEN-20, as validated by TEM, SEM and NTA (Figure 4B). In addition, it also indicates that the
461 proteome of retained EVs is efficiently recovered from the filter for downstream proteomic
462 applications using a lysis buffer containing 5% SDS.

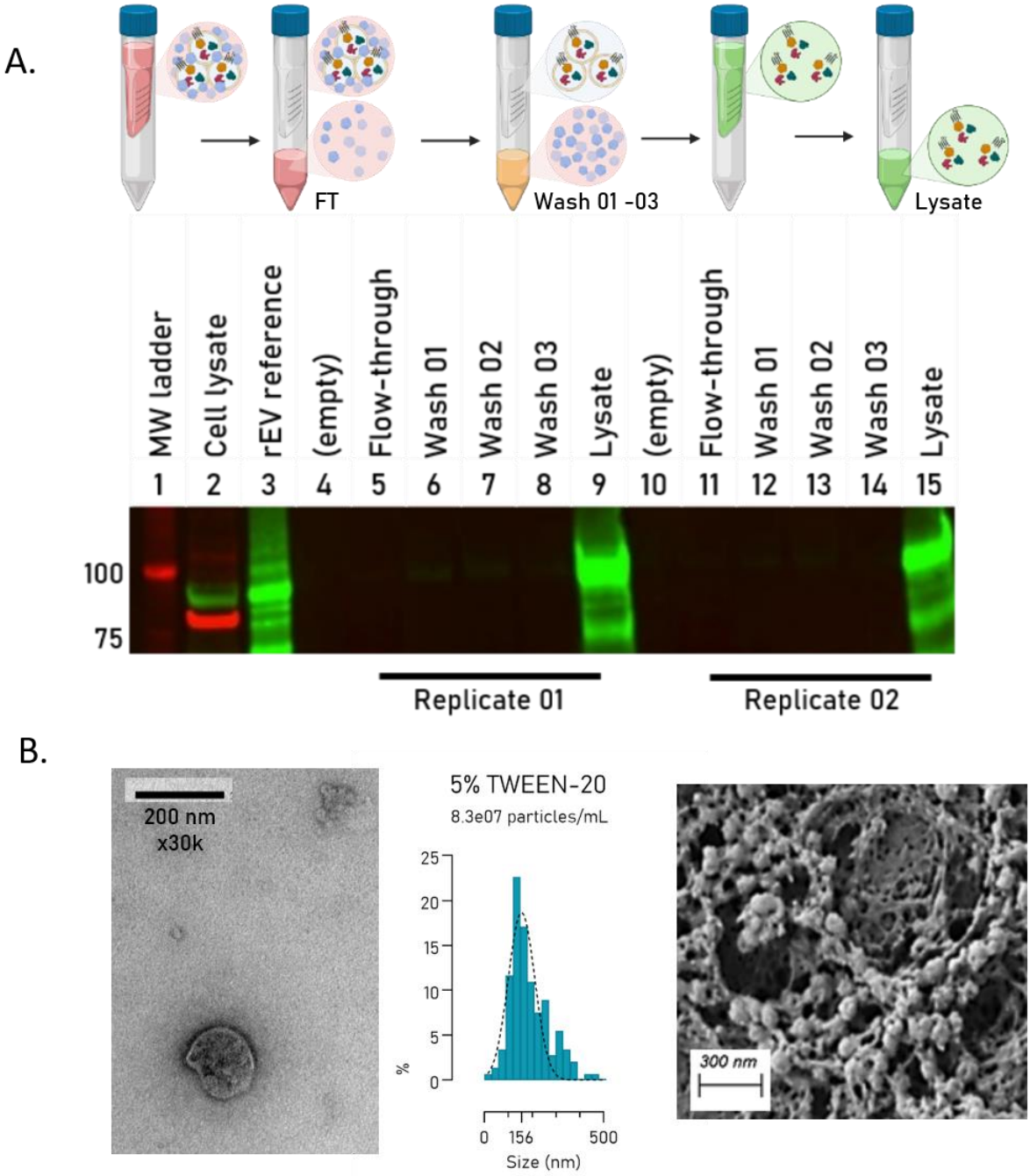

463

464 **Figure 4: The integrity of rEV particles remains even when washing with buffers supplemented**

465 **with 5% TWEEN-20.** A) Western blot of the different fractions during FAEVEr showing that no (or

466 just marginal) luminal Gag-eGFP is observed in the flow-through and wash steps, implying that

467 EVs remain intact. In addition, a strong signal is observed in the lysate fractions, indicating that

468 we can efficiently recover the rEV proteome. B) Qualitative analysis by TEM, NTA and SEM of
469 recovered rEV particles washed in PBS supplemented with 5% TWEEN-20.

470 We further extended our comparison between FAEVEr and UC to evaluate the effect of TWEEN-
471 20 on the purity of the final rEV proteome. We included different percentages of TWEEN-20 in
472 the washing buffer of both FAEVEr and UC and analyzed the corresponding proteomes by LC-
473 MS/MS. We initiated the analysis by comparing the spectral space distribution between human
474 and bovine precursors. Here, we did not only observe a remarkable decrease in bovine
475 precursor intensities using FAEVEr even at the lowest (0.1%) TWEEN-20 concentration, but also
476 that increasing the percentage further improved this (Figure 5A). The effect of supplementing
477 TWEEN-20 is summarized in a principle component analysis (PCA, Figure 5B) which illustrates
478 that supplementing TWEEN-20 has the most drastic change in combination with FAEVEr.

479 Indeed, by combining FAEVER with 5% TWEEN-20, we identified over 3,700 proteins with nearly
480 95% of all PSMs to be of human origin. For UC supplemented with 5% TWEEN-20 in the wash
481 buffer, we also observed an improvement in terms of decreased serum contamination, although
482 not to the same extent, where approximately 80% of the observed precursors were of human
483 origin. Interestingly, we identified over 4,400 proteins in the UC setup, or roughly 15% more
484 proteins in comparison to FAEVEr. We investigated this change in protein abundance further as
485 we expected these extra proteins not all to be serum proteins. We found, by initiating a multiple
486 sample test between the individual experimental setups, (as visualized in the PCA plot) three
487 major groups; UC with or without TWEEN-20, FAEVEr without TWEEN-20 and FAEVEr with
488 TWEEN-20. The setup in which FAEVEr was used without TWEEN-20 appeared to associate with
489 both groups to some extent (Figure 5C). By further examining gene ontology and KEGG terms
490 associated with the corresponding proteins, we found that in FAEVEr supplemented with
491 TWEEN-20, terms including cell-cell adhesion, ESCRT mechanism and (trans)membrane

492 proteins were more abundant (Figure 5D). On the other hand, we noticed that in UC, terms
493 including RNA binding, cell cycle, proteasome and metabolic activities were more prominent
494 (Figure 5E) as well as serum-related terms (e.g. blood microparticle, activation cascade).

495 In conclusion, our results indicate that FAEVEr in combination with TWEEN-20 in the washing
496 buffer improves the overall EV proteome purity, whereas this effect is less prominent in UC.

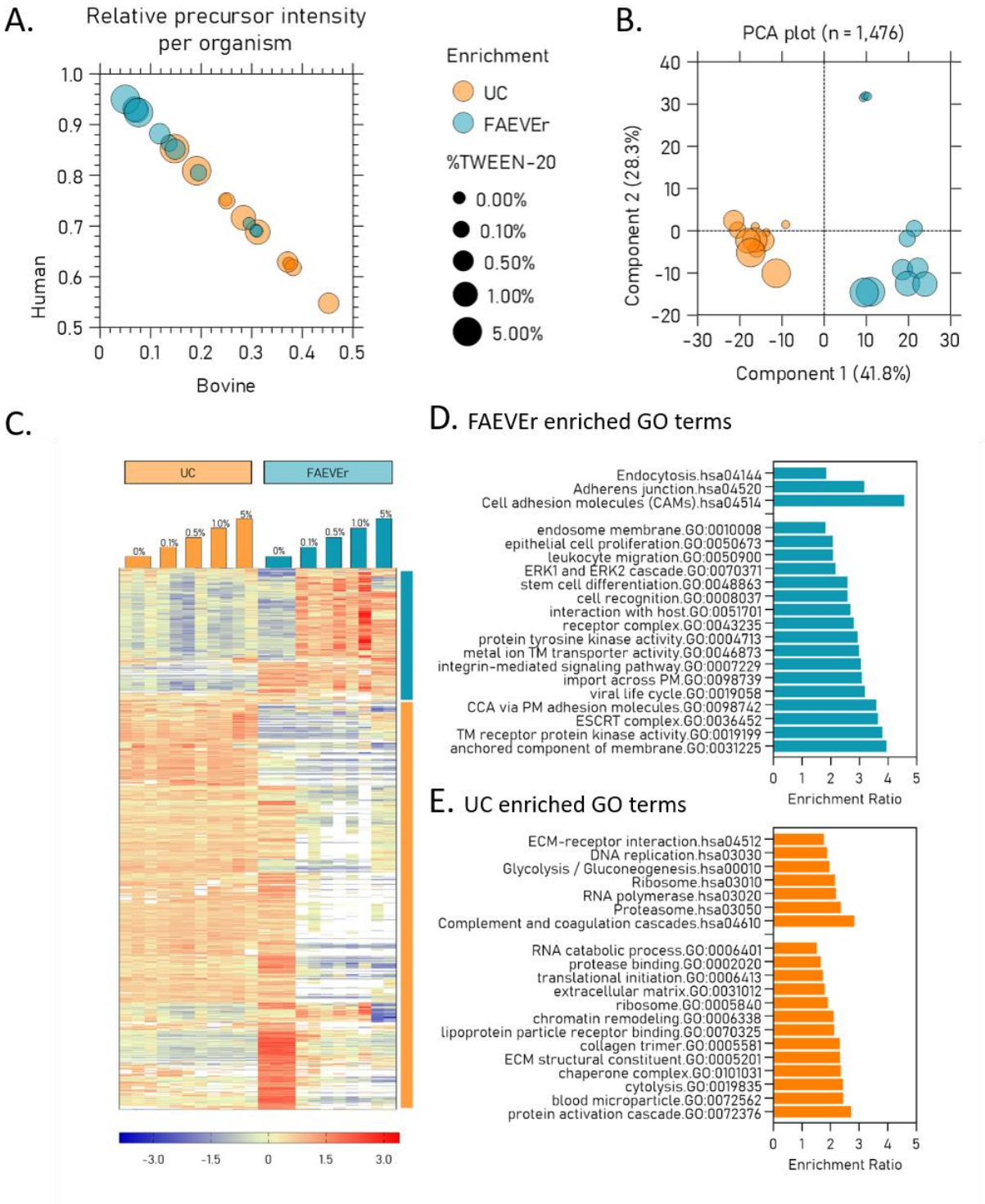

Figure 5: Overview of the effect of TWEEN-20 at different percentages on EV enrichment by UC and FAEVEr. A) Relative share of bovine and human precursor abundance as a measure of

500 serum contamination in function of the enrichment strategy and the percentage of TWEEN-20 in
501 the wash buffer. B) PCA plot of the shared protein intensities between the different experimental
502 setups reveals three major groups. C) Heatmap of the significantly differential abundant proteins
503 (multiple sample test, p-value < 0.05) per experimental setup with the accompanying GO analysis
504 for FAEVEr enriched (D) and UC enriched (E) proteins. UC: ultracentrifugation (orange), FAEVEr:
505 filter-aided EV enrichment (teal), PCA: principal component analysis, GO: Gene ontology, TM:
506 transmembrane, CCA: cell-cell adhesion, ECM: extracellular matrix.

507 ## 4. Effect of serum depletion (on the EV proteome)

508 Fetal bovine serum (FBS) is used as a standard supplement in cell culture media. Unfortunately,
509 it is irreconcilable with EV analysis from conditioned cell media as it contains EVs from bovine
510 origin that interfere with proteome analysis. Therefore, EV depleted serum (EDS) alternatives
511 are used. Consequently, researchers often expand cells for several days in media containing
512 EDS or even refrain from adding serum. To this day, it remains a controversial topic (74) with
513 some researchers advocating against the use of serum because it remains a potential source
514 of xeno-contamination. Others deem serum as an essential supplement for normal cell growth
515 with serum depletion stressing cells due to starvation (75,76), which potentially biases the
516 proteome of the cell culture-derived EVs. Benefiting from the EV-TRACE repository, we noticed
517 that between 2018 and 2023 approximately 56% of the EV experiments that were conducted on
518 conditioned medium of human cell lines were performed using EDS, whereas 30 – 35% of the EV
519 experiments was performed using serum-free conditions.

520 Following the MISEV2018 (7) guidelines, we investigated whether the used EDS is indeed devoid
521 of EV material and addressed this using FAEVEr comparing EDS with FBS. In addition, we

522 examined uses of FBS or EDS had an effect on the cellular and the EV proteome. For these
523 experiments, we made use of MCF7 breast cancer cells.

524 As the high protein concentrations and the accompanying viscosity of serum samples may result
525 in low filtration speed and irreversible blocking of the filter membrane, we diluted the sample
526 three times prior to filtration. After completing the FAEVEr protocol, the proteomes of the
527 FAEVEr filter-retained fraction from commercial FBS and EDS were compared by LC-MS/MS.
528 We validated that EV-specific molecular markers were absent in EDS as well as proteins
529 associated with EV biogenesis. In contrast, these proteins were found abundantly in the FBS
530 retained fraction (**Error! Reference source not found.**).

531 In conclusion, using FAEVEr, we here provide evidence at the LC-MS/MS level that EDS is indeed
532 devoid of EV material and that the FAEVEr strategy is capable of enriching EV particles from
533 complex biological fluids such as (bovine) serum.

534 The protein concentration of serum is reduced by a factor six because of the EV depletion
535 process (**Error! Reference source not found.**A). Indeed, FBS is diluted several times to prevent
536 unintended protein aggregation and pelleting by ultracentrifugation to remove EVs due to the
537 high viscosity of undiluted FBS (73). We decided to explore the effect on the MCF7 cellular
538 proteome once the medium was exchanged from 10% FBS to 10% EDS for 3 days. Besides no
539 change in cell morphology by visual inspection or a significant change in cell count or cell death
540 (**Error! Reference source not found.**B), the LC-MS/MS analysis indicated that only 10 out of more
541 than 7,000 quantified proteins appeared to be significantly differentially regulated between the
542 two conditions (**Error! Reference source not found.**C & 5D). We conclude that shifting from FBS
543 to EDS close to no influence on the viability, growth or proteome of MCF7 cells in culture.

544 We continued investigating the use of FAEVEr by exploring the effect of starvation on the EV
545 proteome by isolating EVs from the conditioned medium of MCF7 cells grown in DMEM
546 supplemented with 0%, 2%, 5% or 10% EDS (D0, D2, D5 and D10, respectively). The FAEVEr retained
547 EVs were purified with wash buffer containing 5% TWEEN-20 and either recovered for NTA
548 (Figure 6A) or lysed for LC-MS/MS analysis. The LC-MS/MS generated data immediately hinted
549 towards an important difference by protein content and quantity between serum-deprived and
550 EDS containing conditions as indicated in the number of identifications (Figure 6B) and the PCA
551 plot (Figure 6C). Over 5,191 proteins were identified in total, from which 4,887 were human and
552 304 were bovine. From the human proteins, 3,610 were found in duplicate in at least one
553 experimental set-up and were included for quantitative comparison of the EV proteomes.
554 Interestingly, we found that only 959 proteins were identified across all samples and that over
555 1,100 proteins were uniquely identified in D0. In addition, we found that the relative abundance of
556 transmembrane proteins gradually increased with increasing levels of EDS, whereas levels of
557 intracellular proteins decreased (Figure 6D). EV markers were abundantly picked-up across the
558 individual samples (Figure 6E). Proteins were then quantitatively compared (multiple sample
559 testing) and hierarchical clustered (Figure 6F) which lead to the conclusion that 333 proteins
560 were significantly differential abundant over two main clusters, between the serum depleted
561 and serum containing conditions. These two clusters were used for gene ontology analysis (GOA)
562 using the Webgestalt v2017 online tool (60). Note that the D0 unique protein list was joined with
563 the proteins that were significantly more abundant in the serum-depleted condition. This GOA
564 analysis revealed that EVs isolated from MCF7 cells cultured in serum-depleted conditions for
565 only 24 h are enriched in proteins involved in metabolism, RNA and DNA binding and autophagy,
566 including organelle fission. Indeed, serum deprived cells are known to rapidly adjust the cellular
567 proteome (**Error! Reference source not found.**), cells are known to upregulate autophagy related
568 (ATG) proteins to replenish essential building blocks and release non-ESCRT dependent

569 exosomes through the formation of autophagosomes (77), which can fuse with endosomes to
570 form amphisomes, similar to MVBs. In addition, the ATG5-ATG16L complex (78,79) influences the
571 EV secretion through dissociation of V-ATPases, thereby preventing MVB acidification and its
572 subsequent lysosomal degradation (80,81). Ultimately, this promotes MVB fusion with the PM
573 and secretion of the ILVs as exosomes. We found that multiple key ATG proteins and contributors
574 of the phagosome biogenesis are high abundant in the EVs isolated from the serum-starved
575 MCF7 cells yet nearly completely absent in the EVs isolated from the serum-containing
576 conditions (Figure 6G & 6H). These findings are in contrast to the serum-containing conditions,
577 where GO terms associated with (trans)membrane proteins (including transmembrane
578 transport, cell-cell adhesion, integrins, vesicle-mediated transport) are enriched as well as
579 proteins associated with the ESCRT complex.

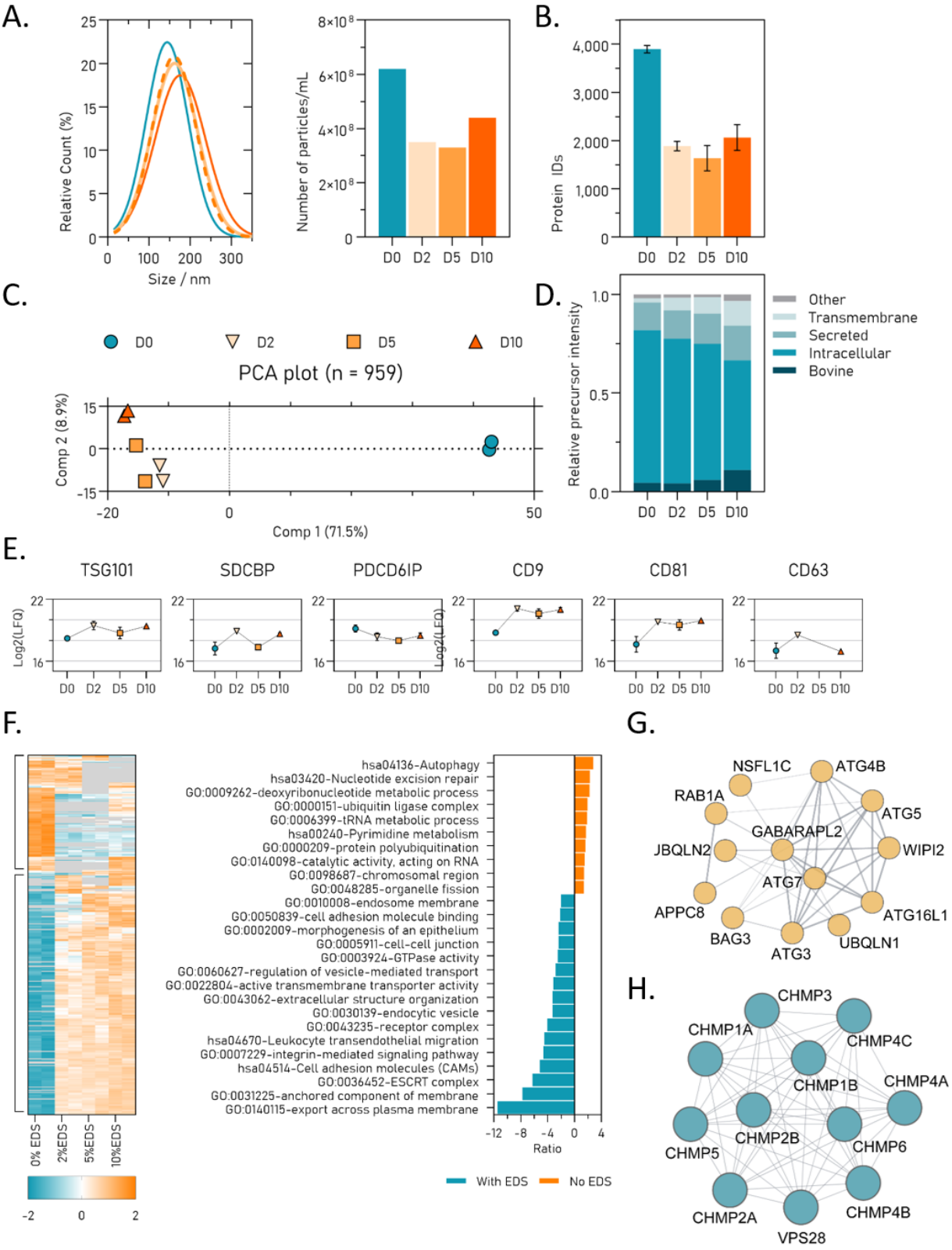
A.
Relative Count (%)
Size / nm
Number of particles/mL
D0 D2 D5 D10
B.
Protein IDs
D0 D2 D5 D10
C.
D0 D2 D5 D10
PCA plot (n = 959)
Comp 2 (8.9%)
Comp 1 (71.5%)
D.
Relative precursor intensity
Other
Transmembrane
Secreted
Intracellular
Bovine
D0 D2 D5 D10
E.
TSG101
SDCBP
PDCD6IP
CD9
CD81
CD63
Log2(LFQ)
D0 D2 D5 D10
F.
0% EDS
2%EDS
5%EDS
10%EDS
hsa04136-Autophagy
hsa03420-Nucleotide excision repair
GO:0009262-deoxyribonucleotide metabolic process
GO:0000151-ubiquitin ligase complex
GO:0006399-tRNA metabolic process
hsa00240-Pyrimidine metabolism
GO:0000209-protein polyubiquitination
GO:0140098-catalytic activity, acting on RNA
GO:0098687-chromosomal region
GO:0048285-organelle fission
GO:0010008-endosome membrane
GO:0050839-cell adhesion molecule binding
GO:0002009-morphogenesis of an epithelium
GO:0005911-cell-cell junction
GO:0003924-GTPase activity
GO:0060627-regulation of vesicle-mediated transport
GO:0022804-active transmembrane transporter activity
GO:0043062-extracellular structure organization
GO:0030139-endocytic vesicle
GO:0043235-receptor complex
hsa04670-Leukocyte transendothelial migration
GO:0007229-integrin-mediated signaling pathway
hsa04514-Cell adhesion molecules (CAMs)
GO:0036452-ESCRT complex
GO:0031225-anchored component of membrane
GO:0140115-export across plasma membrane
Ratio
With EDS
No EDS
G.
NSFL1C
ATG4B
RAB1A
ATG5
GABARAPL2
JBQLN2
WIPI2
ATG7
APPC8
ATG16L1
BAG3
ATG3
UBQLN1
H.
CHMP3
CHMP1A
CHMP4C
CHMP1B
CHMP4A
CHMP5
CHMP2B
CHMP6
CHMP2A
CHMP4B
VPS28

580

581 **Figure 6: Comparison between the EV proteomes isolated from MCF7 cells cultured in different**
582 **percentages of EV-depleted FBS (EDS) reveals drastic changes in protein heterogeneity and**
583 **abundances.** A) NTA analysis of recovered EV particles. B) Number of protein identifications
584 between the conditions. C) PCA plot indicating large variation between the relative abundances
585 of proteins identified in serum-starved (D0) and serum-supplemented conditions (D2, D5 and
586 D10). D) Plot of the localization of the identified proteins. E) Profile plot of six commonly used EV
587 markers. F) Heatmap of the significantly differential abundant proteins between the different
588 conditions and the associated enriched GO terms for serum-starved (orange) and serum-
589 supplemented (teal). Detail of ATG related proteins in the serum-starved condition (G) and the
590 ESCRT associated proteins in the serum-supplemented conditions (H). EDS: EV-depleted FBS;
591 D0, D2, D5 & D10: DMEM supplemented with 0%, 2%, 5% and 10% EDS; NTA: nanoparticle tracking
592 analysis; PCA: principal component analysis; GO: Gene ontology.

593 F. Conclusion and discussion

594 Despite the potential of extracellular vesicles (EVs) for clinical applications such as being a
595 source of circulating biomarkers or therapeutic shuttles, their efficient isolation and purification
596 from complex biofluids in a cost and time efficient manner remains a major bottleneck. Here,
597 we propose filter-aided extracellular vesicle enrichment (FAEVEr) as an EV enrichment strategy
598 that uses 300 kDa MWCO filtration. By combining the filtration steps with wash buffers that
599 contain up to 5% TWEEN-20, we were able to improve the EV proteome purity towards LC-MS/MS
600 compatible levels, even in the presence of 10% EV-depleted FBS (EDS). Recombinant EVs (rEVs,
601 (48,49)) were used to initially establish and optimize our strategy. We made use of the
602 overexpression of a luminal Gag-eGFP construct to evaluate the rEV integrity during the
603 enrichment and purification and concluded that during FAEVEr the rEV particles indeed remain

604 intact. In addition, we concluded that the EVs can be recovered from the filter membrane for
605 further evaluation using common tools for EV characterization such as nanoparticle tracking
606 analysis (NTA) and scanning and transmission electron microscopy (SEM and TEM). In addition,
607 the rEV proteome was quantitatively recovered by immediately lysing the filter-retained EVs for
608 LC-MS/MS analysis and we identified over 5,000 human HEK293T proteins from 1 mL conditioned
609 medium. Amongst these proteins we found the different EV markers next to multiple
610 (trans)membrane proteins and proteins associated with EV biogenesis, which underlines the
611 potential of FAEVEr for EV proteomics.

612 We benchmarked our approach against ultracentrifugation (UC), a widespread implemented
613 method for EV enrichment, and showed that over 95% of the protein identifications overlap.
614 Furthermore, we found an increase in EV purity following FAEVEr compared to
615 ultracentrifugation as demonstrated by a reduced fraction of the LC-MS/MS spectral space
616 taken by bovine precursors, thereby limiting the competitive effect towards the identification of
617 low abundant (EV) proteins. In addition, we observed a drastic decrease in the relative variance
618 (%CV) between the number of identifications on both the protein, peptide and peptide-spectral
619 match level between UC and FAEVEr. This also indicates a higher reproducibility between
620 replicates, which in turn leads to improved data completeness (fewer missing values) and,
621 consequently, improved quantifications. We hypothesize that this improvement is due to the
622 absence of intermediate pipetting steps that remove the supernatant after ultracentrifugation,
623 which potentially leads to incomplete removal or unintended perturbations of the EV pellet. In
624 FAEVEr however, we create a distinct separation between the EV depleted filtrate and EV
625 enriched retentate, thereby omitting unnecessary pipetting steps, as the filtrate is simply
626 decanted.

627 We continued to improve the EV purity by implementing TWEEN-20 in wash buffers as this
628 detergent was previously shown not to lyse EVs, even in relatively high concentrations (67), and
629 it is an established supplement to reduce non-specific protein-membrane interactions, for
630 example in Western blotting. We provide insights in the gradual loss of bovine serum proteins
631 and secreted proteins, to which we refer here as non-EV proteins. This improved removal of
632 unwanted proteins is of high importance for LC-MS/MS based bottom-up proteomics, as
633 precursors from such high abundant proteins (e.g. albumin) dominate the spectral space,
634 outcompeting relevant EV precursors. Surprisingly, we observed that supplementing TWEEN-20
635 to the wash step of UC did not have the same profound effect compared to FAEVEr. Indeed, a
636 number of proteins associated with (amongst others) transcription and translation, proteasomal
637 degradation and metabolic activities were more prominent in all ultracentrifugation samples as
638 well as in the FAEVEr setup without TWEEN-20 supplemented to the wash buffers. In contrast,
639 the TWEEN-20 washed EV proteomes following the FAEVEr protocol were enriched in
640 (trans)membrane proteins and in proteins from the ESCRT machinery. We hypothesize that
641 during cell culture inevitable cell lysis occurs during which cytosolic proteins are released and
642 co-purified during ultracentrifugation. These insights raise the question whether or not such
643 proteins are effectively encapsulated in EVs or if they form non-specific protein interactions
644 with the EV membrane. However, additional studies are required to confirm this.

645 In EV research, many experiments exclude serum supplements in cell culture media to repulse
646 xeno-proteins and omit the suppressive competitive effect during LC-MS/MS analysis and the
647 potential biological influence on the EV proteomics outcome. We first investigated on the
648 difference between regular FBS and EV-depleted FBS (EDS) on the LC-MS/MS level, from which
649 we concluded that EV markers and biogenesis related proteins are virtually absent in EDS,
650 implying that we do not contaminate our EV preparation unintendedly with bovine EV particles.

651 We further elaborate that the depletion of serum during cell culture, even for a limited period of
652 time (e.g. 24 h), has a dramatic effect on the EV proteome of MCF7 cells. In line with Leidal *et al.*
653 (77) we observed an increase in protein heterogeneity associated with RNA binding,
654 biosynthesis, cell cycle and autophagy, pointing towards an alternative biogenesis of EV
655 particles through the formation of amphisomes. These findings are underlined by the unique
656 presence of several ATG proteins in the EV preparation of serum-starved MCF7 cells. In contrast
657 to this, the EV proteome from MCF7 cells supplemented with EV-depleted FBS, contained higher
658 levels of proteins associated with transmembrane transport, cell-cell adhesion and the ESCRT-
659 machinery were more abundant. We feel that the choice to add or exclude EDS during cell culture
660 for EV research is an important consideration when testing a preconceived hypothesis as it may
661 bias the interpretation of the EV (proteomics) data (82,83).

662 Our data shows that filter-aided EV enrichment, FAEVEr, using 300 kDa MWCO PES filters is an
663 efficient strategy to isolate EVs from complex medium and that, by including TWEEN-20, we
664 further improved the overall purity of the EV proteome without affecting the EV integrity, even
665 at relatively high TWEEN-20 concentrations. Furthermore, FAEVEr is conducted in a relatively
666 short timeframe and it offers the possibility of parallelization using standard lab equipment. In
667 comparison, ultracentrifugation is limited to six or ten samples and requires at least two rounds
668 of centrifugation.

669

670 G. Supplemental figures legends

671 **Supplementary Figure 1: Schematic overview of the expression of GAG-eGFP in HEK293T cells.**
672 Top: HEK293T cells are transfected with a Gag-eGFP construct, encoding for a Gag-eGFP fusion

673 protein that multimerizes at the endosomal and plasma membrane, inducing the formation of
674 virus-like particles packed with eGFP. Bottom: brightfield and eGFP pictures of HEK293T cells
675 after transfection, prior to the isolation of conditioned medium.

676 **Supplementary Figure 2: Scanning electron microscopy of 300 kDa MWCO filters used in FAEVEr.**
677 Blank: empty filter membrane with clear visualization of the 300 kDa MWCO filter membrane.
678 Synthetic particles: homogeneous synthetic particles used for NTA calibration were retained on
679 the filter after completing the FAEVEr protocol and serve as a positive control. rEV: retained rEV
680 particles after completing the FAEVEr protocol with a distinct delineation of the EV particles
681 against the 300 kDa MWCO membrane.

682 **Supplementary Figure 3: SDS-PAGE with Coomassie staining indicates quantitative removal of**
683 **serum proteins with FAEVEr when TWEEN-20 is supplemented to the filter, indicating decreased**
684 **membrane fouling.** In the PBS condition (no TWEEN-20) a faint band is observed at 65 kDa,
685 indicating that only a fraction of the bovine albumin is removed by the wash steps. This stands
686 in contrast to washing with buffers that are supplemented with of TWEEN-20, where more
687 intense bands are observed in the washes. Additionally, the lysate of PBS contains observable
688 more albumin material, further indicating that PBS alone fails to remove the bulk of
689 contaminants contrary to TWEEN-20 were the lysate does not contain such strong signal.

690 **Supplementary Figure 4: Comparison of the identified proteins in standard fetal bovine serum**
691 **(FBS) and EV-depleted FBS (EDS).** A) After completing FAEVEr and subjecting the lysate to LC-
692 MS/MS analysis, we observed a high number of identifications in FBS but not in EDS, indicating
693 a higher protein heterogeneity due to the presence of EV particles. B) EV markers or biogenesis
694 related proteins are virtually absent in EDS, yet highly abundant in FBS.

695 **Supplementary Figure 5: Culturing MCF7 cells in 10% standard fetal bovine serum (FBS) or 10%**
696 **EV-depleted FBS (EDS) for three days, has no huge effect on the MCF7 cellular proteome.** A)
697 Due to the EV depletion protocol, EDS contains approximately six times less protein material. B)
698 No significant changes in cell viability or cell count were observed. C) In both conditions, we
699 identified over 7,000 proteins from which only 10 were significantly differentially regulated (D).

700 **Supplementary Figure 6: The cellular proteome of MCF7 cells cultured at different percentages**
701 **of EV-depleted FBS (EDS) changes between serum-starved (0% EDS for 24 h) and optimal**
702 **conditions (10% EDS for 48 h).** A) Heatmap depicting the differentially regulated proteins between
703 the different conditions from which we further investigated two major clusters to evaluate the
704 contrast between 0% EDS and 10% EDS. Gene ontology (GO) analysis of the proteins up-regulated
705 in the serum-starved conditions (B) and optimal conditions (C).

706 H. List of abbreviations

707 DDA: Data dependent acquisition

708 DIA: Data independent acquisition

709 EC: extracellular

710 EDS: EV-depleted FBS

711 ESCRT: endosomal sorting complexes required for transport

712 EV: extracellular vesicle

713 FAEVEr: Filter-aided extracellular vesicle enrichment

714 FBS: fetal bovine serum

715 GO: Gene ontology

716 ILV: inter-luminal vesicles

717 LC-MS/MS: Liquid chromatography coupled tandem mass spectrometry

718 LFQ: label-free quantification

719 MVB: multivesicular body

720 MWCO: molecular weight cut-off

721 NTA: nanoparticle tracking analysis

722 PCA: principal component analysis

723 PES: Polyethersulfone

724 PM: plasma membrane

725 PSM: peptide-spectral match

726 rEV: recombinant EV

727 SDS: sodium dodecyl sulphate

728 SEC: size-exclusion chromatography

729 SEM: scanning electron microscopy

730 TEM: transmission electron microscopy

731 UC: ultracentrifugation

732 %CV: coefficient of variance

733 ## I. Ethical approval

734 Not applicable

735 ## J. Consent for publications

736 All co-authors have consented to publication

737 ## K. Data availability

738 The mass spectrometry proteomics data have been deposited to the ProteomeXchange
739 Consortium via the PRIDE partner repository with the dataset identifiers PXD051938 (comparison
740 FAEVEr with UC), PXD051955 (comparison MCF7 proteome of EVs and cells under starving
741 conditions) and PXD051956 (comparison FBS with EDS). All required details concerning the
742 enrichment of extracellular vesicles were submitted to EV-TRACK (EV240045).

743 ## L. Competing interest

744 The authors declare no conflict of interest.

745 ## M. Funding statement

746 K.G. and S.E. acknowledge support by a Strategic Basic Research project (EV-TRACE) from the
747 Research Foundation -Flanders (FWO), project number S006319N.

748 ## N. Author contributions

749 JP planned, designed and performed the experiments and wrote the manuscript. JVDV, FDM and
750 DDP assisted with the experiments. TVDS performed the HEK293T cell culture and production of

751 rEV material. FB performed the electron microscopy. All authors read and approved the
752 manuscript.

753 O. Acknowledgements

754 The authors thank all operators of the VIB Proteomics Core for their excellence and input. The
755 authors thank the lab of An Hendrix for kindly providing us with the required purified rEV
756 aliquots.

757 P. References

758 1. Dixson AC, Dawson TR, Di Vizio D, Weaver AM. Context-specific regulation of extracellular
759 vesicle biogenesis and cargo selection. Nat Rev Mol Cell Biol. 2023 Jul 1;24(7):454–76.

760 2. van Niel G, D'Angelo G, Raposo G. Shedding light on the cell biology of extracellular vesicles.
761 Nat Rev Mol Cell Biol. 2018 Apr 1;19(4):213–28.

762 3. Colombo M, Moita C, van Niel G, Kowal J, Vigneron J, Benaroch P, et al. Analysis of ESCRT
763 functions in exosome biogenesis, composition and secretion highlights the heterogeneity of
764 extracellular vesicles. J CELL Sci. 2013 Dec 15;126(24):5553–65.

765 4. Wei D, Zhan W, Gao Y, Huang L, Gong R, Wang W, et al. RAB31 marks and controls an ESCRT-
766 independent exosome pathway. Cell Res. 2021 Feb 1;31(2):157–77.

767 5. Mathieu M, Martin-Jaular L, Lavieu G, Théry C. Specificities of secretion and uptake of
768 exosomes and other extracellular vesicles for cell-to-cell communication. Nat Cell Biol. 2019
769 Jan 1;21(1):9–17.

770 6. Yu L, Zhu G, Zhang Z, Yu Y, Zeng L, Xu Z, et al. Apoptotic bodies: bioactive treasure left behind
771 by the dying cells with robust diagnostic and therapeutic application potentials. J
772 Nanobiotechnology. 2023 Jul 12;21(1):218.

773 7. Théry C, Witwer KW, Aikawa E, Alcaraz MJ, Anderson JD, Andriantsitohaina R, et al. Minimal
774 information for studies of extracellular vesicles 2018 (MISEV2018): a position statement of the
775 International Society for Extracellular Vesicles and update of the MISEV2014 guidelines. J
776 Extracell Vesicles. 2018 Dec 1;7(1):1535750.

777 8. Cocucci E, Meldolesi J. Ectosomes and exosomes: shedding the confusion between
778 extracellular vesicles. Trends Cell Biol. 2015 Jun 1;25(6):364–72.

779 9. Hadisurya M, Lee ZC, Luo Z, Zhang G, Ding Y, Zhang H, et al. Data-Independent Acquisition
780 Phosphoproteomics of Urinary Extracellular Vesicles Enables Renal Cell Carcinoma Grade
781 Differentiation. Mol Cell Proteomics. 2023 May 1;22(5):100536.

10. Hoshino A, Costa-Silva B, Shen TL, Rodrigues G, Hashimoto A, Tesic Mark M, et al. Tumour exosome integrins determine organotropic metastasis. Nature. 2015 Nov 1;527(7578):329–35.

11. Joshi BS, de Beer MA, Giepmans BNG, Zuhorn IS. Endocytosis of Extracellular Vesicles and Release of Their Cargo from Endosomes. ACS Nano. 2020 Apr 28;14(4):4444–55.

12. Stahl PD, Raposo G. Extracellular Vesicles: Exosomes and Microvesicles, Integrators of Homeostasis. Physiology. 2019 May 1;34(3):169–77.

13. Takahashi A, Okada R, Nagao K, Kawamata Y, Hanyu A, Yoshimoto S, et al. Exosomes maintain cellular homeostasis by excreting harmful DNA from cells. Nat Commun. 2017 May 16;8(1):15287.

14. Amin S, Massoumi H, Tewari D, Roy A, Chaudhuri M, Jazayerli C, et al. Cell Type-Specific Extracellular Vesicles and Their Impact on Health and Disease. Int J Mol Sci. 2024;25(5).

15. Hánělová K, Raudenská M, Masařík M, Balvan J. Protein cargo in extracellular vesicles as the key mediator in the progression of cancer. Cell Commun Signal. 2024 Jan 10;22(1):25.

16. Hoffmann O, Wormland S, Bittner AK, Collenburg M, Horn PA, Kimmig R, et al. Programmed death receptor ligand-2 (PD-L2) bearing extracellular vesicles as a new biomarker to identify early triple-negative breast cancer patients at high risk for relapse. J Cancer Res Clin Oncol. 2023 Mar 1;149(3):1159–74.

17. Zhang XW, Qi GX, Liu MX, Yang YF, Wang JH, Yu YL, et al. Deep Learning Promotes Profiling of Multiple miRNAs in Single Extracellular Vesicles for Cancer Diagnosis. ACS Sens [Internet]. 2024 Mar 5; Available from: https://doi.org/10.1021/acssensors.3c02789

18. Dorado E, Doria ML, Nagelkerke A, McKenzie JS, Maneta-Stavrakaki S, Whittaker TE, et al. Extracellular vesicles as a promising source of lipid biomarkers for breast cancer detection in blood plasma. J Extracell Vesicles. 2024 Mar 1;13(3):e12419.

19. Ma D, Xie A, Lv J, Min X, Zhang X, Zhou Q, et al. Engineered extracellular vesicles enable high-efficient delivery of intracellular therapeutic proteins. Protein Cell. 2024 Mar 22;pwae015.

20. Attem J, Narayana RVL, Manukonda R, Kaliki S, Vemuganti GK. Small extracellular vesicles loaded with carboplatin effectively enhance the cytotoxicity of drug-resistant cells from Y79 cells-in vitro. Biomed Pharmacother. 2024 Apr 1;173:116403.

21. Lone SN, Nisar S, Masoodi T, Singh M, Rizwan A, Hashem S, et al. Liquid biopsy: a step closer to transform diagnosis, prognosis and future of cancer treatments. Mol Cancer. 2022 Mar 18;21(1):79.

22. K S, T D, M P. Small extracellular vesicles as a multicomponent biomarker platform in urinary tract carcinomas. Front Mol Biosci [Internet]. 2022;9. Available from: https://www.frontiersin.org/articles/10.3389/fmolb.2022.916666

23. Gao X, Gao B, Li S. Extracellular vesicles: A new diagnostic biomarker and targeted drug in osteosarcoma. Front Immunol [Internet]. 2022;13. Available from: https://api.semanticscholar.org/CorpusID:252468251

24. Hirschberg Y, Valle-Tamayo N, Dols-Icardo O, Engelborghs S, Buelens B, Vandenbroucke RE, et al. Proteomic comparison between non-purified cerebrospinal fluid and cerebrospinal

fluid-derived extracellular vesicles from patients with Alzheimer's, Parkinson's and Lewy body dementia. J Extracell Vesicles. 2023 Dec 1;12(12):12383.

25. Vandendriessche C, Kapogiannis D, Vandenbroucke RE. Biomarker and therapeutic potential of peripheral extracellular vesicles in Alzheimer's disease. Adv Drug Deliv Rev. 2022 Nov 1;190:114486.

26. Newman LA, Muller K, Rowland A. Circulating cell-specific extracellular vesicles as biomarkers for the diagnosis and monitoring of chronic liver diseases. Cell Mol Life Sci. 2022 Apr 10;79(5):232.

27. Mazzucco M, Mannheim W, Shetty SV, Linden JR. CNS endothelial derived extracellular vesicles are biomarkers of active disease in multiple sclerosis. Fluids Barriers CNS. 2022 Feb 8;19(1):13.

28. Horvatovich PL, Bischoff R. Current Technological Challenges in Biomarker Discovery and Validation. Eur J Mass Spectrom. 2010 Feb 1;16(1):101–21.

29. Schiess R, Wollscheid B, Aebersold R. Targeted proteomic strategy for clinical biomarker discovery. Mol Oncol. 2009 Feb 1;3(1):33–44.

30. Burton JB, Carruthers NJ, Stemmer PM. Enriching extracellular vesicles for mass spectrometry. Mass Spectrom Rev. 2023 Mar 1;42(2):779–95.

31. Demichev V, Messner CB, Vernardis SI, Lilley KS, Ralser M. DIA-NN: neural networks and interference correction enable deep proteome coverage in high throughput. Nat Methods. 2020 Jan 1;17(1):41–4.

32. Gessulat S, Schmidt T, Zolg DP, Samaras P, Schnatbaum K, Zerweck J, et al. Prosit: proteome-wide prediction of peptide tandem mass spectra by deep learning. Nat Methods. 2019 Jun 1;16(6):509–18.

33. Guzman UH, Martinez-Val A, Ye Z, Damoc E, Arrey TN, Pashkova A, et al. Ultra-fast label-free quantification and comprehensive proteome coverage with narrow-window data-independent acquisition. Nat Biotechnol [Internet]. 2024 Feb 1; Available from: https://doi.org/10.1038/s41587-023-02099-7

34. Yoshitake J, Azami M, Sei H, Onoshima D, Takahashi K, Hirayama A, et al. Rapid Isolation of Extracellular Vesicles Using a Hydrophilic Porous Silica Gel-Based Size-Exclusion Chromatography Column. Anal Chem. 2022 Oct 11;94(40):13676–81.

35. Vanderboom PM, Dasari S, Ruegsegger GN, Pataky MW, Lucien F, Heppelmann CJ, et al. A size-exclusion-based approach for purifying extracellular vesicles from human plasma. Cell Rep Methods. 2021 Jul 26;1(3):100055.

36. Onódi Z, Pelyhe C, Terézia Nagy C, Brenner GB, Almási L, Kittel Á, et al. Isolation of High-Purity Extracellular Vesicles by the Combination of Iodixanol Density Gradient Ultracentrifugation and Bind-Elute Chromatography From Blood Plasma. Front Physiol [Internet]. 2018;9. Available from: https://www.frontiersin.org/journals/physiology/articles/10.3389/fphys.2018.01479

37. Gallart-Palau X, Serra A, Wong ASW, Sandin S, Lai MKP, Chen CP, et al. Extracellular vesicles are rapidly purified from human plasma by PRotein Organic Solvent PRecipitation (PROSPR). Sci Rep. 2015 Sep 30;5(1):14664.

862 38. Rider MA, Hurwitz SN, Meckes DG. ExtraPEG: A Polyethylene Glycol-Based Method for
863 Enrichment of Extracellular Vesicles. Sci Rep. 2016 Apr 12;6(1):23978.

864 39. Brambilla D, Sola L, Ferretti AM, Chiodi E, Zarovni N, Fortunato D, et al. EV Separation:
865 Release of Intact Extracellular Vesicles Immunocaptured on Magnetic Particles. Anal Chem.
866 2021 Apr 6;93(13):5476–83.

867 40. Vergauwen G, Tulkens J, Pinheiro C, Avila Cobos F, Dedeyne S, De Scheerder MA, et al.
868 Robust sequential biophysical fractionation of blood plasma to study variations in the
869 biomolecular landscape of systemically circulating extracellular vesicles across clinical
870 conditions. J Extracell Vesicles. 2021 Aug 1;10(10):e12122.

871 41. Van Dorpe S, Lippens L, Boiy R, Pinheiro C, Vergauwen G, Rappu P, et al. Integrating automated
872 liquid handling in the separation workflow of extracellular vesicles enhances specificity and
873 reproducibility. J Nanobiotechnology. 2023 May 19;21(1):157.

874 42. An M, Wu J, Zhu J, Lubman DM. Comparison of an Optimized Ultracentrifugation Method
875 versus Size-Exclusion Chromatography for Isolation of Exosomes from Human Serum. J
876 Proteome Res. 2018 Oct 5;17(10):3599–605.

877 43. Turner NP, Abeysinghe P, Kwan Cheung KA, Vaswani K, Logan J, Sadowski P, et al. A
878 Comparison of Blood Plasma Small Extracellular Vesicle Enrichment Strategies for
879 Proteomic Analysis. Proteomes. 2022;10(2).

880 44. Brennan K, Martin K, FitzGerald SP, O'Sullivan J, Wu Y, Blanco A, et al. A comparison of
881 methods for the isolation and separation of extracellular vesicles from protein and lipid
882 particles in human serum. Sci Rep. 2020 Jan 23;10(1):1039.

883 45. Baranyai T, Herczeg K, Onódi Z, Voszka I, Módos K, Marton N, et al. Isolation of Exosomes
884 from Blood Plasma: Qualitative and Quantitative Comparison of Ultracentrifugation and Size
885 Exclusion Chromatography Methods. PLOS ONE. 2015 Dec 21;10(12):e0145686.

886 46. Askeland A, Borup A, Østergaard O, Olsen JV, Lund SM, Christiansen G, et al. Mass-
887 Spectrometry Based Proteome Comparison of Extracellular Vesicle Isolation Methods:
888 Comparison of ME-kit, Size-Exclusion Chromatography, and High-Speed Centrifugation.
889 Biomedicines. 2020;8(8).

890 47. Van Deun J, Mestdagh P, Agostinis P, Akay Ö, Anand S, Anckaert J, et al. EV-TRACK:
891 transparent reporting and centralizing knowledge in extracellular vesicle research. Nat
892 Methods. 2017 Mar 1;14(3):228–32.

893 48. Geeurickx E, Lippens L, Rappu P, De Geest BG, De Wever O, Hendrix A. Recombinant
894 extracellular vesicles as biological reference material for method development, data
895 normalization and assessment of (pre-)analytical variables. Nat Protoc. 2021 Feb 1;16(2):603–
896 33.

897 49. Geeurickx E, Tulkens J, Dhondt B, Van Deun J, Lippens L, Vergauwen G, et al. The
898 generation and use of recombinant extracellular vesicles as biological reference material.
899 Nat Commun. 2019 Jul 23;10(1):3288.

900 50. Sidhom K, Obi PO, Saleem A. A Review of Exosomal Isolation Methods: Is Size Exclusion
901 Chromatography the Best Option? Int J Mol Sci. 2020;21(18).

902 51. Ding M, Wang C, Lu X, Zhang C, Zhou Z, Chen X, et al. Comparison of commercial exosome
903 isolation kits for circulating exosomal microRNA profiling. Anal Bioanal Chem. 2018 Jun
904 1;410(16):3805–14.

905 52. Royo F, Zuñiga-Garcia P, Sanchez-Mosquera P, Egia A, Perez A, Loizaga A, et al. Different
906 EV enrichment methods suitable for clinical settings yield different subpopulations of urinary
907 extracellular vesicles from human samples. J Extracell Vesicles. 2016 Jan 1;5(1):29497.

908 53. Lobb RJ, Becker M, Wen Wen S, Wong CSF, Wiegmans AP, Leimgruber A, et al. Optimized
909 exosome isolation protocol for cell culture supernatant and human plasma. J Extracell
910 Vesicles. 2015 Jan 1;4(1):27031.

911 54. Guan S, Yu H, Yan G, Gao M, Sun W, Zhang X. Characterization of Urinary Exosomes
912 Purified with Size Exclusion Chromatography and Ultracentrifugation. J Proteome Res. 2020
913 Jun 5;19(6):2217–25.

914 55. Gámez-Valero A, Monguió-Tortajada M, Carreras-Planella L, Franquesa M, Beyer K,
915 Borràs FE. Size-Exclusion Chromatography-based isolation minimally alters Extracellular
916 Vesicles' characteristics compared to precipitating agents. Sci Rep. 2016 Sep 19;6(1):33641.

917 56. Vergauwen G, Dhondt B, Van Deun J, De Smedt E, Berx G, Timmerman E, et al.
918 Confounding factors of ultrafiltration and protein analysis in extracellular vesicle research.
919 Sci Rep. 2017 Jun 2;7(1):2704.

920 57. Jordan KR, Hall JK, Schedin T, Borakove M, Xian JJ, Dzieciatkowska M, et al. Extracellular
921 vesicles from young women's breast cancer patients drive increased invasion of non-
922 malignant cells via the Focal Adhesion Kinase pathway: a proteomic approach. Breast Cancer
923 Res. 2020 Nov 23;22(1):128.

924 58. Allelein S, Medina-Perez P, Lopes ALH, Rau S, Hause G, Kölsch A, et al. Potential and
925 challenges of specifically isolating extracellular vesicles from heterogeneous populations.
926 Sci Rep. 2021 Jun 2;11(1):11585.

927 59. Eyckerman S, Titeca K, Van Quickelberghe E, Cloots E, Verhee A, Samyn N, et al. Trapping
928 mammalian protein complexes in viral particles. Nat Commun. 2016 Apr 28;7(1):11416.

929 60. Wang J, Vasaikar S, Shi Z, Greer M, Zhang B. WebGestalt 2017: a more comprehensive,
930 powerful, flexible and interactive gene set enrichment analysis toolkit. Nucleic Acids Res. 2017
931 Jul 3;45(W1):W130–7.

932 61. HaileMariam M, Eguez RV, Singh H, Bekele S, Ameni G, Pieper R, et al. S-Trap, an Ultrafast
933 Sample-Preparation Approach for Shotgun Proteomics. J Proteome Res. 2018 Sep
934 7;17(9):2917–24.

935 62. Ono A. HIV-1 assembly at the plasma membrane: Gag trafficking and localization. Future
936 Virol. 2009 May 1;4(3):241–57.

937 63. Chhuon C, Zhang SY, Jung V, Lewandowski D, Lipecka J, Pawlak A, et al. A sensitive S-
938 Trap-based approach to the analysis of T cell lipid raft proteome. J Lipid Res. 2020 Nov
939 1;61(11):1512–23.

940 64. Elinger D, Gabashvili A, Levin Y. Suspension Trapping (S-Trap) Is Compatible with Typical
941 Protein Extraction Buffers and Detergents for Bottom-Up Proteomics. J Proteome Res. 2019
942 Mar 1;18(3):1441–5.

943 65. Ludwig KR, Schroll MM, Hummon AB. Comparison of In-Solution, FASP, and S-Trap
944 Based Digestion Methods for Bottom-Up Proteomic Studies. J Proteome Res. 2018 Jul
945 6;17(7):2480–90.

946 66. Varnavides G, Madern M, Anrather D, Hartl N, Reiter W, Hartl M. In Search of a Universal
947 Method: A Comparative Survey of Bottom-Up Proteomics Sample Preparation Methods. J
948 Proteome Res. 2022 Oct 7;21(10):2397–411.

949 67. Osteikoetxea X, Sódar B, Németh A, Szabó-Taylor K, Pálóczi K, Vukman KV, et al.
950 Differential detergent sensitivity of extracellular vesicle subpopulations. Org Biomol Chem.
951 2015;13(38):9775–82.

952 68. Osteikoetxea X, Balogh A, Szabó-Taylor K, Németh A, Szabó TG, Pálóczi K, et al. Improved
953 Characterization of EV Preparations Based on Protein to Lipid Ratio and Lipid Properties.
954 PLOS ONE. 2015 Mar 23;10(3):e0121184.

955 69. Choi DS, Kim DK, Kim YK, Gho YS. Proteomics, transcriptomics and lipidomics of
956 exosomes and ectosomes. PROTEOMICS. 2013 May 1;13(10–11):1554–71.

957 70. Subra C, Laulagnier K, Perret B, Record M. Exosome lipidomics unravels lipid sorting at
958 the level of multivesicular bodies. Recent Dev Biosynth Storage Transp Lipids. 2007 Feb
959 1;89(2):205–12.

960 71. Minhua Feng, Berdugo Morales A, Poot A, Beugeling T, Bantjes A. Effects of Tween 20 on the
961 desorption of proteins from polymer surfaces. J Biomater Sci Polym Ed. 1996 Jan 1;7(5):415–
962 24.

963 72. Amirilargani M, Saljoughi E, Mohammadi T. Improvement of permeation performance of
964 polyethersulfone (PES) ultrafiltration membranes via addition of Tween-20. J Appl Polym Sci.
965 2010 Jan 5;115(1):504–13.

966 73. Lee KJ, Mower R, Hollenbeck T, Castelo J, Johnson N, Gordon P, et al. Modulation of
967 Nonspecific Binding in Ultrafiltration Protein Binding Studies. Pharm Res. 2003 Jul
968 1;20(7):1015–21.

969 74. Urzì O, Olofsson Bagge R, Crescitelli R. The dark side of foetal bovine serum in
970 extracellular vesicle studies. J Extracell Vesicles. 2022 Oct 1;11(10):e12271.

971 75. Drabovich AP, Pavlou MP, Dimitromanolakis A, Diamandis EP. Quantitative Analysis of
972 Energy Metabolic Pathways in MCF-7 Breast Cancer Cells by Selected Reaction Monitoring
973 Assay *. Mol Cell Proteomics. 2012 Aug 1;11(8):422–34.

974 76. Nie S, McDermott SP, Deol Y, Tan Z, Wicha MS, Lubman DM. A quantitative proteomics
975 analysis of MCF7 breast cancer stem and progenitor cell populations. PROTEOMICS. 2015 Nov
976 1;15(22):3772–83.

977 77. Leidal AM, Huang HH, Marsh T, Solvik T, Zhang D, Ye J, et al. The LC3-conjugation
978 machinery specifies the loading of RNA-binding proteins into extracellular vesicles. Nat Cell
979 Biol. 2020 Feb 1;22(2):187–99.

980 78. Fujita N, Itoh T, Omori H, Fukuda M, Noda T, Yoshimori T. The Atg16L Complex Specifies
981 the Site of LC3 Lipidation for Membrane Biogenesis in Autophagy. Mol Biol Cell. 2008 May
982 1;19(5):2092–100.

983 79. Matsushita M, Suzuki NN, Obara K, Fujioka Y, Ohsumi Y, Inagaki F. Structure of Atg5·Atg16,
984 a Complex Essential for Autophagy *. J Biol Chem. 2007 Mar 2;282(9):6763–72.

985 80. Urbańska K, Orzechowski A. The Secrets of Alternative Autophagy. Cells. 2021;10(11).

986 81. Salimi L, Akbari A, Jabbari N, Mojarad B, Vahhabi A, Szafert S, et al. Synergies in exosomes
987 and autophagy pathways for cellular homeostasis and metastasis of tumor cells. Cell Biosci.
988 2020 May 13;10(1):64.

989 82. Pirkmajer S, Chibalin AV. Serum starvation: caveat emptor. Am J Physiol-Cell Physiol.
990 2011 Aug 1;301(2):C272–9.

991 83. Shin J, Rhim J, Kwon Y, Choi SY, Shin S, Ha CW, et al. Comparative analysis of differentially
992 secreted proteins in serum-free and serum-containing media by using BONCAT and pulsed
993 SILAC. Sci Rep. 2019 Feb 28;9(1):3096.

994

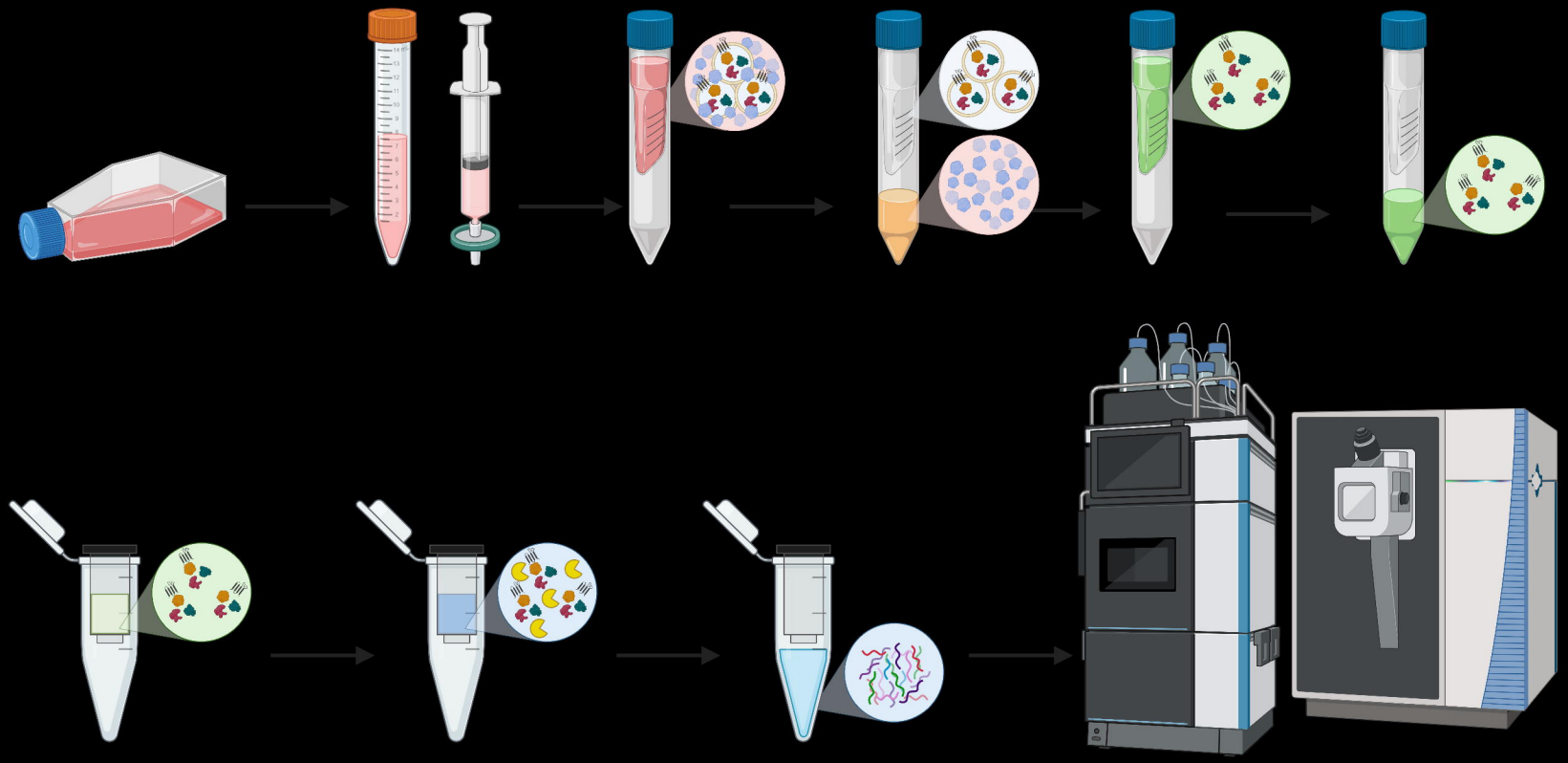

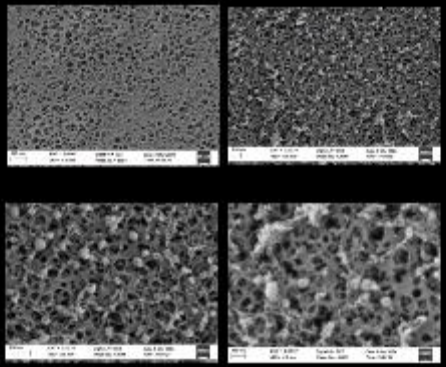

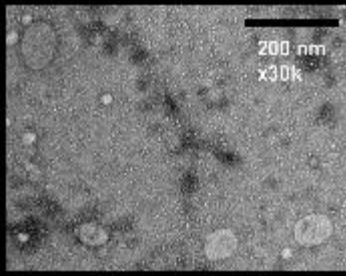
200 nm
x30k

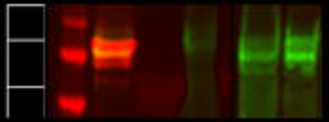

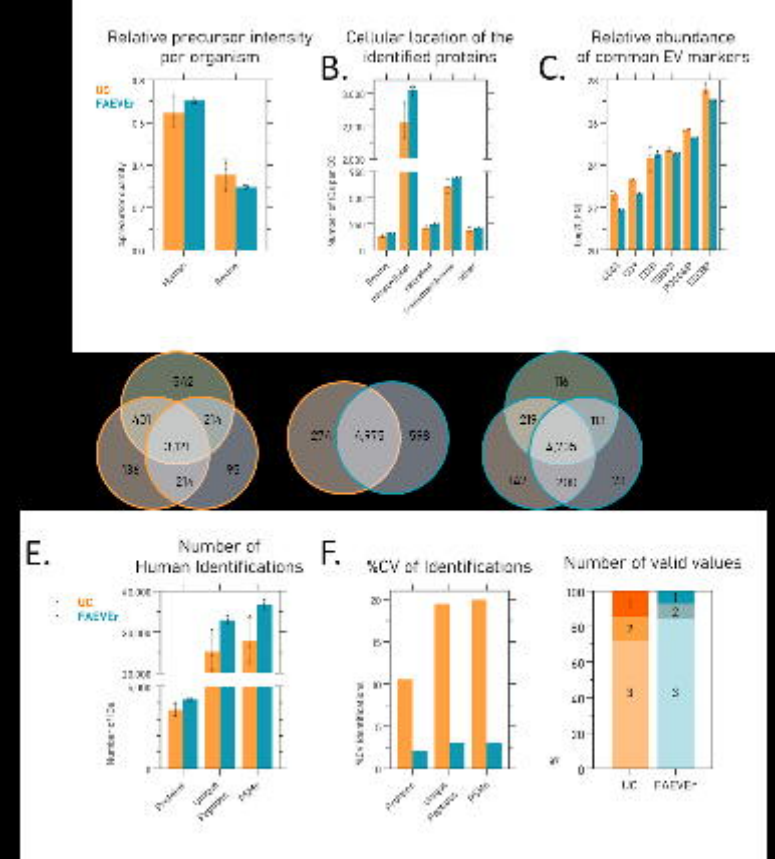
Relative precursor intensity per organism
UC
FAEVEr
B.
Cellular location of the identified proteins
C.
Relative abundance of common EV markers
E.
Number of Human Identifications
UC
FAEVEr
F.
%CV of Identifications
Number of valid values
UC
FAEVEr

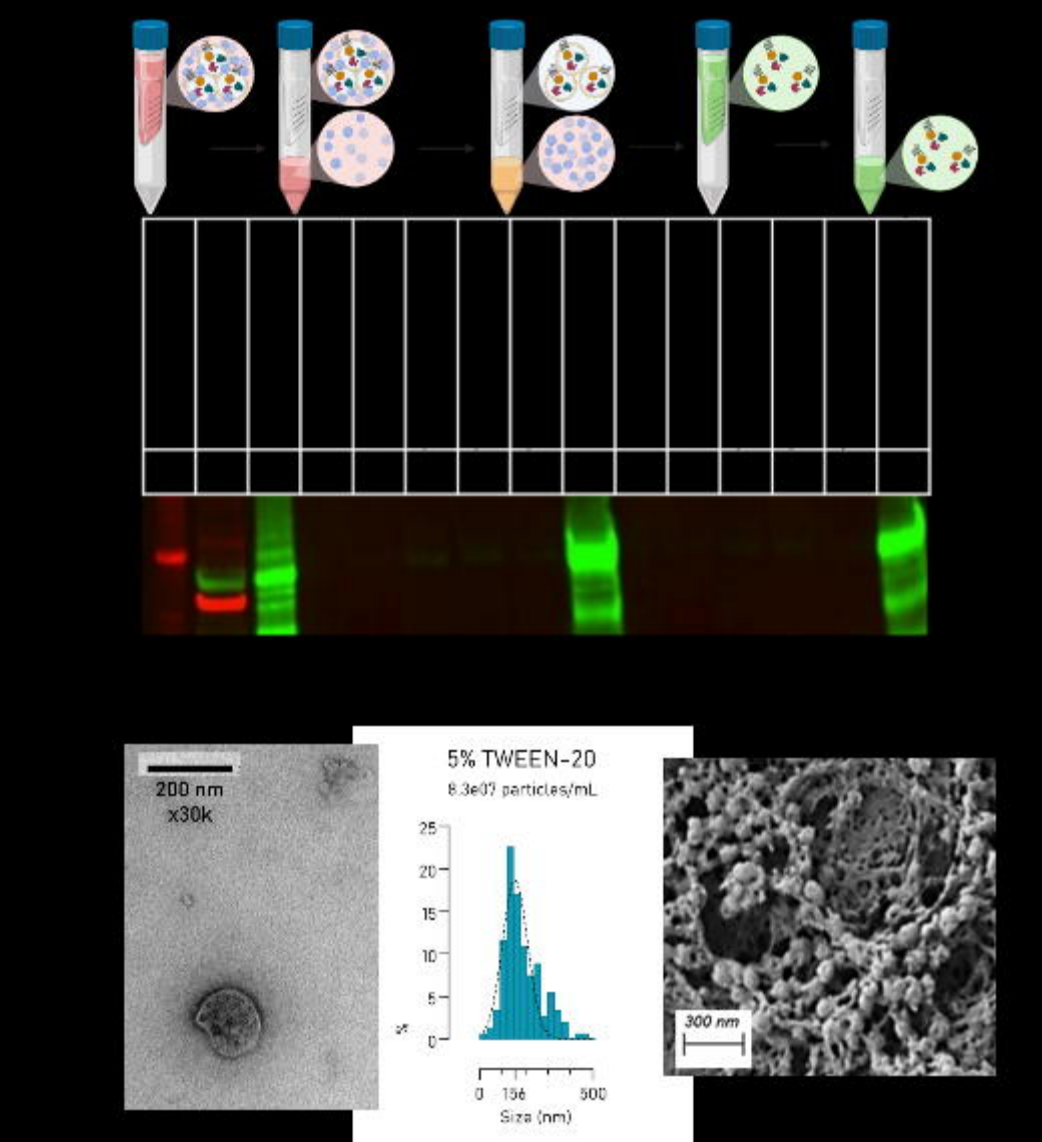
200 nm
x30k
5% TWEEN-20
8.3e07 particles/mL
25
20
15
10
5
0
%
0
156
500
Size (nm)
300 nm

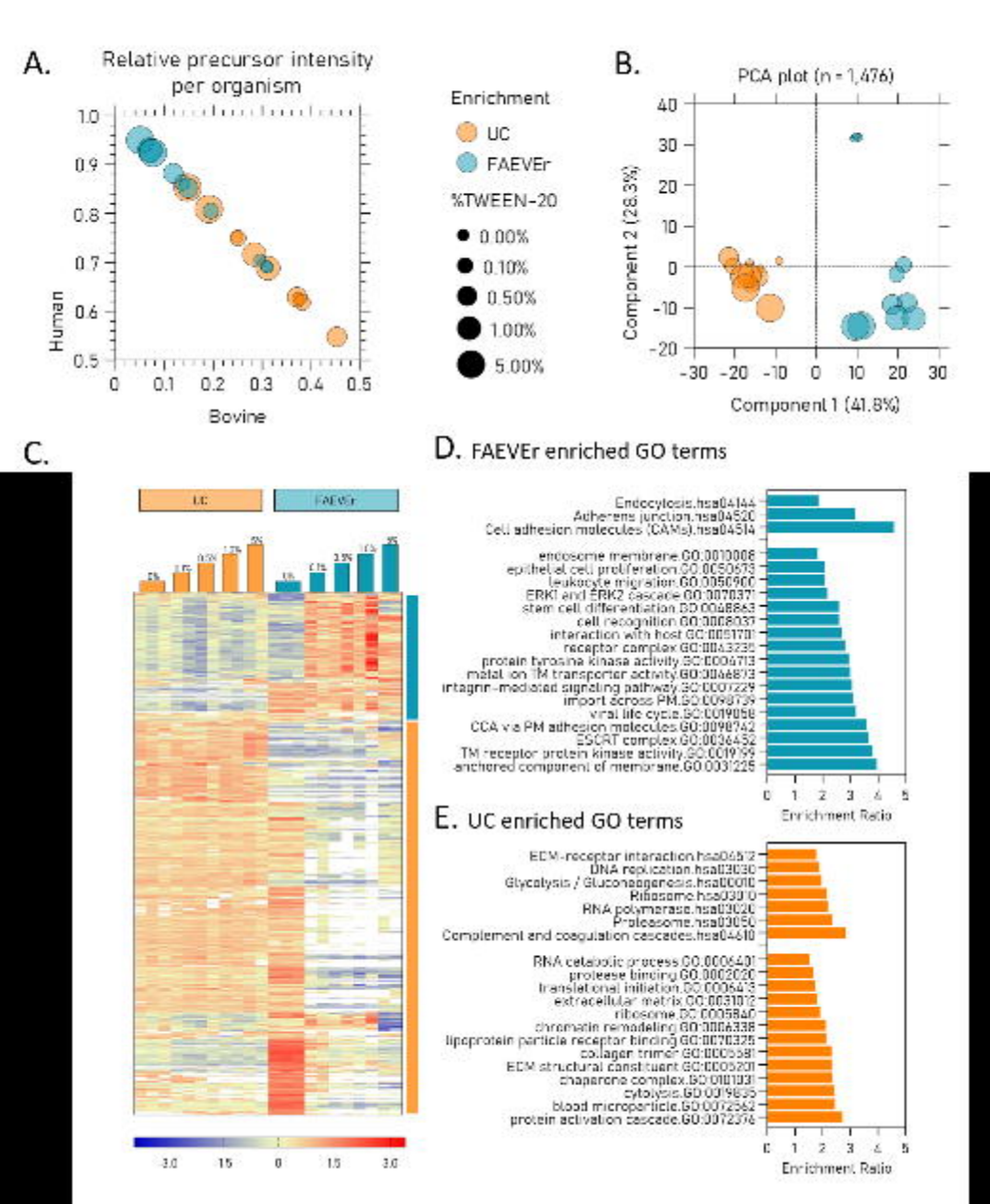
A.
Relative precursor intensity per organism
Human
Bovine
Enrichment
UC
FAEVEr
%TWEEN-20
0.00%
0.10%
0.50%
1.00%
5.00%
B.
PCA plot (n = 1,476)
Component 2 (28.3%)
Component 1 (41.8%)
C.
UC
FAEVEr
D. FAEVEr enriched GO terms
Endocytosis.hsa04144
Adherens junction.hsa04520
Cell adhesion molecules (CAMs).hsa04514
endosome membrane.GO:0010008
epithelial cell proliferation.GO:0050673
leukocyte migration.GO:0050900
ERK1 and ERK2 cascade.GO:0070371
stem cell differentiation.GO:0048863
cell recognition.GO:0008037
interaction with host.GO:0051701
receptor complex.GO:0043235
protein tyrosine kinase activity.GO:0004713
metal ion TM transporter activity.GO:0046873
integrin-mediated signaling pathway.GO:0007229
import across PM.GO:0098739
viral life cycle.GO:0019058
CCA via PM adhesion molecules.GO:0098742
ESCRT complex.GO:0036452
TM receptor protein kinase activity.GO:0019199
anchored component of membrane.GO:0031225
Enrichment Ratio
E. UC enriched GO terms
ECM-receptor interaction.hsa04512
DNA replication.hsa03030
Glycolysis / Gluconeogenesis.hsa00010
Ribosome.hsa03010
RNA polymerase.hsa03020
Proteasome.hsa03050
Complement and coagulation cascades.hsa04610
RNA catabolic process.GO:0006401
protease binding.GO:0002020
translational initiation.GO:0006413
extracellular matrix.GO:0031012
ribosome.GO:0005840
chromatin remodeling.GO:0006338
lipoprotein particle receptor binding.GO:0070325
collagen trimer.GO:0005581
ECM structural constituent.GO:0005201
chaperone complex.GO:0101031
cytolysis.GO:0019835
blood microparticle.GO:0072562
protein activation cascade.GO:0072376
Enrichment Ratio

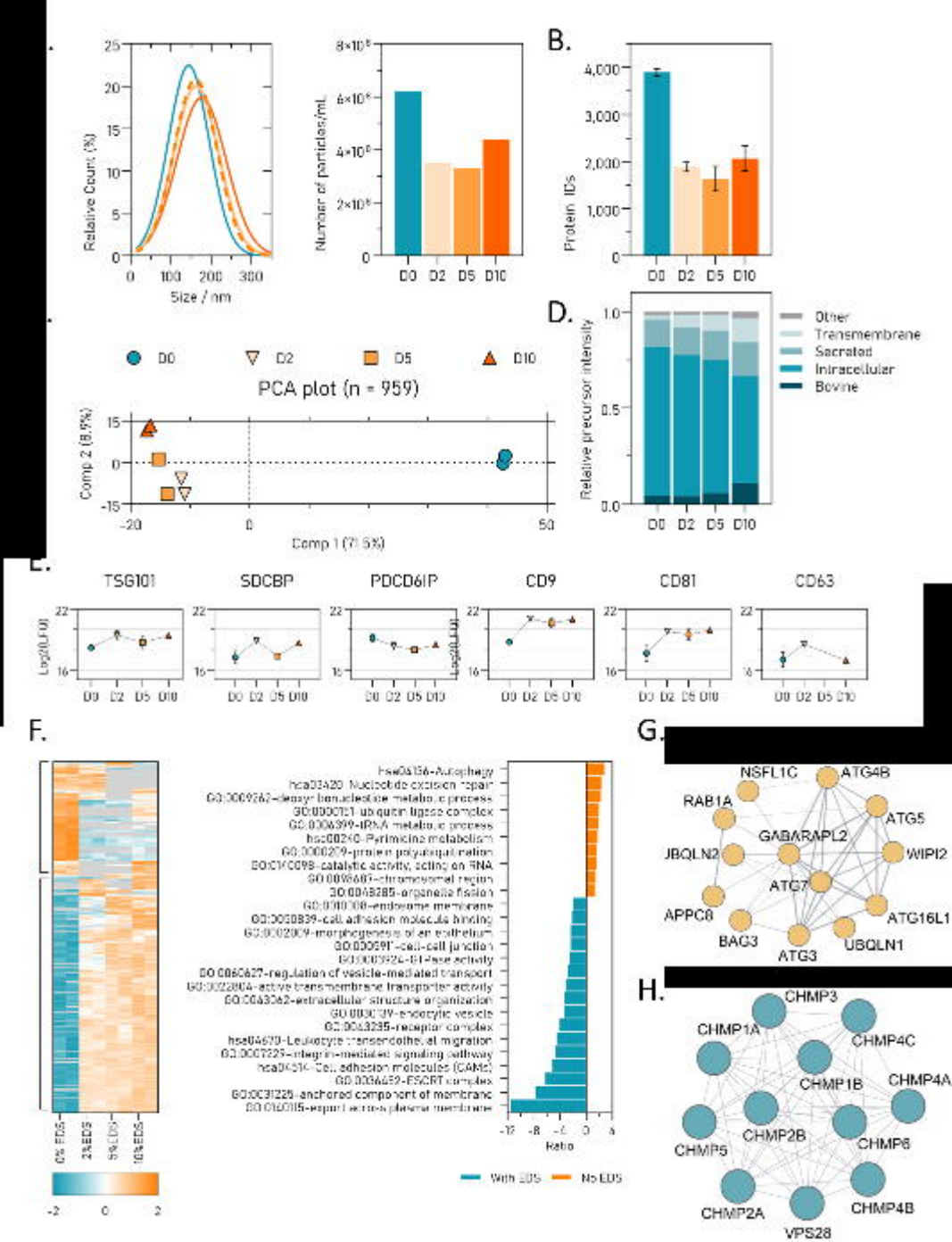
Relative Count (%)
Size / nm
Number of particles/mL
B.
Protein IDs
D0 D2 D5 D10
D0 D2 D5 D10
PCA plot (n = 959)
Comp 2 (8.5%)
Comp 1 (71.5%)
D.
Relative precursor intensity
Other
Transmembrane
Secreted
Intracellular
Bovine
E.
TSG101
SDCBP
PDCD6IP
CD9
CD81
CD63
Log2(LFQ)
F.
0% EDS
2% EDS
5% EDS
10% EDS
Ratio
With EDS
No EDS
G.
NSFL1C
ATG4B
RAB1A
ATG5
GABARAPL2
JBQLN2
WIPI2
ATG7
APPC6
ATG16L1
BAG3
ATG3
UBQLN1
H.
CHMP3
CHMP1A
CHMP4C
CHMP1B
CHMP4A
CHMP2B
CHMP5
CHMP6
CHMP2A
CHMP4B
VPS28